Establishing virtual bioequivalence and clinically relevant specifications using *in vitro* biorelevant dissolution testing and physiologically-based population pharmacokinetic modeling. Case example: Naproxen

Authors: Ioannis Loisios-Konstantinidis[1], Rodrigo Cristofoletti[2], Nikoletta Fotaki[3], David B. Turner[5], Jennifer Dressman[1,4]

Author Information:

[1] Institute of Pharmaceutical Technology, Goethe University, Frankfurt am Main, Germany,

[2] Center for Pharmacometrics and Systems Pharmacology, Department of Pharmaceutics, College of Pharmacy, University of Florida, Orlando, Florida, USA.

[3] Department of Pharmacy and Pharmacology, Faculty of Science, University of Bath, Bath, UK,

[4] Fraunhofer IME - Translational Pharmacology and Medicine, Carl-von-Noorden Platz 9, Frankfurt am Main, Germany

[5] Certara UK Limited, Simcyp Division, 1 Concourse Way, Sheffield S1 2BJ, United Kingdom

Correspondence:

Jennifer Dressman, Biocenter, Institute of Pharmaceutical Technology, Johann Wolfgang Goethe University, Max-von-Laue-Str. 9, Frankfurt am Main 60438, Germany. Email: dressman@em.uni-frankfurt.de

Abstract:

Background: Physiologically-based population pharmacokinetic modeling (popPBPK) coupled with *in vitro* biopharmaceutics tools such as biorelevant dissolution testing can serve as a powerful tool to establish virtual bioequivalence and set clinically relevant specifications. One of several applications of popPBPK modeling is in the emerging field of virtual bioequivalence (VBE), where it can be used to streamline drug development by implementing model-informed formulation design and to inform regulatory decision-making e.g., with respect to evaluating the possibility of extending BCS-based biowaivers beyond BCS Class I and III compounds in certain cases.

Methods: In this study, Naproxen, a BCS class II weak acid was chosen as the model compound. *In vitro* biorelevant solubility and dissolution experiments were performed and the resulting data were used as an input to the PBPK model, following a stepwise workflow for the confirmation of the biopharmaceutical parameters. The naproxen PBPK model was developed by implementing a middle-out approach and verified against clinical data obtained from the literature. Once confidence in the performance of the model was achieved, several *in vivo* dissolution scenarios, based on model-based analysis of the *in vitro* data, were used to simulate clinical trials in healthy adults. Inter-occasion variability (IOV) was also added to critical *physiological* parameters and mechanistically propagated through the simulations. The various trials were simulated on a "worst/best case" dissolution scenario and average bioequivalence was assessed according to C_{max}, AUC and t_{max}.

Results: VBE results demonstrated that naproxen products with *in vitro* dissolution reaching 85% dissolved within 90 minutes would lie comfortably within the bioequivalence limits for C_{max} and AUC. Based on the establishment of VBE, a dissolution "safe space" was designed and a clinically relevant specification for naproxen products was proposed. The interplay between formulation-related and drug-specific PK parameters (e.g., t1/2) to predict the *in vivo* performance was also investigated.

Conclusion: Over a wide range of values, the *in vitro* dissolution rate is not critical for the clinical performance of naproxen products and therefore naproxen could be eligible for BCS-based biowaivers

based on *in vitro* dissolution under intestinal conditions. This approach may also be applicable to other poorly soluble acidic compounds with long half-lives, providing an opportunity to streamline drug development and regulatory decision-making without putting the patient at a risk.

Key words: PBPK, modeling & simulation; virtual bioequivalence; IVIVE, clinically relevant specifications; dissolution safe-space; biorelevant dissolution

Table of Contents

89

90

1 Introduction

Physiologically-based population pharmacokinetic (popPBPK) modelling has been implemented successfully to support and inform drug product development and regulatory decision-making.(Babiskin and Zhang, 2015; Doki et al., 2017; Heimbach et al., n.d.; Mitra, 2019; Olivares-Morales et al., 2016; Parrott et al., 2014; Pepin et al., 2016; Stillhart et al., 2017; Suarez-Sharp et al., 2018; Zhang et al., 2017) Patient-centric, model-informed drug product development necessitates an *in vitro-in vivo-in silico* link to establish clinically relevant specifications and thus guarantee the quality of the drug product with respect to safety and efficacy. By encompassing model-informed formulation selection and prediction of clinical performance, modeling and simulation (M & S) provides a way forward to the design of "safe spaces", and thus offer regulatory relief. Some examples include guiding development of biorelevant and/or biopredictive dissolution methods to support biowaiver extensions and enabling extrapolation to special populations (e.g., paediatrics). Although the current PBPK regulatory guidelines still mainly focus on the prediction of drug-drug interactions (DDIs),(European Medicines Agency (EMA), 2018a; U.S.FDA Center for Drug Evaluation and Research (CDER), 2018a) the integration of translational biopharmaceutical modeling and dissolution testing has been attracting increased attention from leading pharmaceutical industries as well as regulatory bodies and over the last few years, the regulatory impact of mechanistic absorption modeling has significantly increased.(Babiskin and Zhang, 2015; Heimbach et al., 2019; Pepin et al., 2016; Zhang et al., 2017)

Establishing bioequivalence (BE) has been a critical component of and remains a challenge during development of both new drug and generic products. In the context of quality by design (QbD) and the biopharmaceutics risk assessment roadmap (BioRAM),(Selen et al., 2014)·(Dickinson et al., 2008) the importance of linking *in vitro* with *in vivo* data bi-directionally has received greater emphasis. Accordingly, virtual bioequivalence (VBE) can serve as a powerful tool to set clinically relevant

specifications and predict anticipated clinical outcomes in healthy, patient and special-patient (e.g., paediatrics and/ or co-administration of PPIs) populations. To accurately predict the *in vivo* performance of a drug product through clinical trial simulation, a certain set of conditions needs to be met. This includes integration of biorelevant *in vitro* data into the simulation model as well as mechanistic absorption modelling, disposition/elimination components and consideration of physiological and physicochemical interactions with the formulation. After developing the mechanistic absorption PBPK model, it must be verified via learn/ confirm cycles which rely on evaluation against observed clinical data. Such models can then be used to predict the population pharmacokinetic variability of the test drug/ formulation and therefore enable assessment of bioequivalence risks via virtual trials simulations.(Pathak et al., 1997)

The ability of PBPK to account for between-subject (BS), within-subject (WS) and inter-occasion variability (IOV) is crucial to the accuracy and the applicability of VBE results. Although the current techniques can address the between-subject variability reasonably well, progress still needs to be made in the area of estimating inter-occasion variability. Two independent modeling strategies to incorporate IOV in VBE studies have been implemented in the literature: a) *a priori* estimated random error terms in replicate clinical study are added to the PK parameters, or, more mechanistically, b) the IOV is integrated into the system parameters and propagated in simulations.(Wedagedera et al., 2017)

In this study, an *in vitro-in vivo-in silico* workflow to establish VBE and clinically relevant dissolution specifications is proposed. Naproxen and its sodium salt was chosen as the case example. Naproxen is a weakly acidic (pK_a ≈4.4) non-steroid anti-inflammatory (NSAID) agent. It is a biopharmaceutical classification system (BCS) class II weak acid with poor solubility in the fasted stomach but freely soluble in the intestinal environment and has a high permeability, similar to ibuprofen and diclofenac.(Cristofoletti et al., 2013; Cristofoletti and Dressman, 2016; Kambayashi et al., 2013) Since the absorption of such compounds is usually complete, they have been identified as offering opportunities for a potential BCS-based biowaiver extension.(Cristofoletti and Dressman, 2016; Tubic-Grozdanis et al., 2008; Yazdanian et al., 2004) The free acid (Naprosyn®) and the sodium salt

(Anaprox®) forms are administered orally as immediate release (IR) tablets. The purpose of this article is to characterize the *in vitro* dissolution behavior of naproxen pure API and formulations, integrate mechanistic absorption modeling with population-based PBPK, design a safe space and, last but not least, set clinically relevant dissolution specifications through VBE trials. The possibility/ risk of granting BCS-biowaiver for naproxen products is also investigated.

2 Material and Methods

2.1 Chemicals and reagents

Naproxen (lot #SLBV2253) and naproxen sodium (lot #MKCD6021) pure active pharmaceutical ingredient (API) were purchased commercially from Sigma-Aldrich Co., LLC. (St. Louis, MO). Naproxen tablets (500 mg Naprosyn®, lot 70662; Minerva Pharmaceutical Inc., Athens, Greece) and naproxen sodium tablets (550 mg Anaprox®, lot 70466; Minerva Pharmaceutical Inc., Athens, Greece) were commercially purchased from the Greek market. Fasted state simulated gastric fluid (FaSSGF)/fasted state simulated intestinal fluid (FaSSIF V1)/fed state simulated intestinal fluid (FeSSIF V1) powder (lot 01-1512-05NP), FeSSIF V2 powder (lot 03-1610-02) and FaSSIF V3 powder (lot PHA S 1306023) were kindly donated from Biorelevant.com Ltd., (Surrey, UK). Acetonitrile (lot 18A101551) and water (lot 17B174006) of HPLC-grade were from VWR Chemicals (Leuven, Belgium). Sodium hydroxide pellets (lot 14A100027), sodium chloride (lot 17I074122), sodium acetate (lot 14B240013), hydrochloric acid 37% (lot 10L060526), orthophosphoric acid 85% (lot 12K210017) and glacial acetic acid 100% (lot 12B220508) were commercially obtained from VWR Chemicals (Leuven, Belgium). Sodium dihydrogen phosphate dehydrate (lot K93701642712), maleic acid (lot 57118880544) and citric acid (lot

K91221207425) were commercially purchased from Merck KGaA (Darmstadt, Germany). Pepsin from pocrine gastric mucosa 19.6% and Lipofundin® MCT/LCT 20% were from Sigma-Aldrich Co., LLC. (St. Louis, MO) and B. Braun Melsungen AG (Melsungen, Germany), respectively.

2.2 *In vitro* solubility experiments

The solubility of naproxen and its sodium salt was investigated in various selected aqueous and biorelevant dissolution media using the Uniprep™ system (Whatman®, Piscataway, NJ, USA). All aqueous buffers were prepared according to the European Pharmacopoeia, while the biorelevant media were prepared according to Markopoulos et al. and Fuchs et al.(Fuchs et al., 2015; Markopoulos et al., 2015) The composition and physicochemical characteristics of the fasted and fed state biorelevant media used in this study are summarized in Table 1. An excess amount of API was added to 3 mL of dissolution medium and the samples were incubated for 24 h at 37˚C on an orbital mixer. The samples were then filtered through the 0.45 µm PTFE filter integrated in the Uniprep™ system. The filtrate was immediately diluted with mobile phase and analyzed by high-performance liquid chromatography (HPLC) (see section 2.5). All measurements were performed at least in triplicate (n≥3).

Table 1: Composition and physicochemical characteristics of biorelevant media in the fasted and fed states.

2.3 *In vitro* dissolution tests

All dissolution tests were performed using calibrated USP II (paddle) apparatus (Erweka DT 80, Heusenstamm, Germany) at 37±0.4˚C. Each vessel contained 500 mL of fresh, pre-warmed medium

and the rotational speed was set at 75 rpm. Samples were withdrawn at 2.5, 5, 10, 15, 20, 30, 45, 60, 90 and 120 minutes via a 5 mL glass syringe connected to a stainless-steel cannula containing a 10 µm polyethylene cannula filter. Immediately thereafter, the sample was filtered through a 0.45 µm PTFE filter (ReZist™ 30, GE Healthcare UK Ltd., Buckinghamshire, UK), discarding the first 2 mL. The filtrate was immediately diluted with mobile phase and analyzed by HPLC-UV (see section 2.5). The removal of 5 mL at each sampling time was taken into account in the calculation of the percentage dissolved. All experiments were performed at least in triplicate (n≥3) and the final pH in the vessel was recorded.

2.4 Two-stage dissolution tests

Since the conventional one-stage USP II dissolution test does not include a gastric compartment to account for disintegration of the dosage form in the stomach, differences in the disintegration time between non-coated (i.e. 500 mg Naprosyn®) and simple coated formulation (i.e. 550 mg Anaprox®) might bias the interpretation of the biorelevant *in vitro* dissolution behavior with respect to the *in vivo* performance. Therefore, to investigate the disintegration effect on the *in vitro* performance of naproxen/ naproxen sodium formulations, a two-stage dissolution test for FaSSIF V3 was developed based on the publication by Mann et al. (Mann et al., 2017)

The dosage form was initially exposed to 250 mL of FaSSGF Level III and samples were removed at 5, 10, 15, 20, 30 minutes and treated as described in section 2.3. After the withdrawal of the last sample, 6.8 mL of sodium hydroxide 1M and immediately thereafter 250 mL of FaSSIF V3 concentrate pH=6.7 (double concentration of all the constituents, apart from sodium hydroxide) were added to the vessel. Instead of increasing the pH of the intestinal medium concentrate to counterbalance the acidic pH of the stomach medium as described in the original study,(Mann et al., 2017) sodium hydroxide was added first, but almost simultaneously, with the FaSSIF V3 concentrate. This was done to avoid using a very high pH in the FaSSIF V3 concentrate. After addition of sodium hydroxide and concentrated

FaSSIF V3, further samples were removed at 32.5, 35, 40, 45, 50, 60 and 90 minutes. The two-stage experiments were performed using calibrated USP II (paddle) apparatus (Erweka DT 80, Heusenstamm, Germany) at 37±0.4˚C and the samples were analyzed by HPLC-UV (see section 2.5). All experiments were performed at least in triplicate (n≥3) and the final pH in the vessel was recorded.

2.5 Quantitative Analysis of Samples

Samples obtained from solubility and dissolution experiments were first filtered through a 0.45 µm PTFE filter (ReZist™ 30 syringe filter or Uniprep™; Whatman®, Piscataway, NJ, USA) and subsequently, after appropriate dilution with mobile phase, they were analyzed by HPLC-UV (Hitachi Chromaster; Hitachi Ltd., Tokyo, Japan or Spectra System HPLC, ThermoQuest Inc., San Jose, USA). A BDS Hypersil C18, 5 µm, 150 x 4.6 mm (Thermo Scientific) analytical column combined with a pre-column (BDS Hypersil C-18, 3µm, 10 x 4mm) was used. The mobile phase consisted of 20 mM NaH_2PO_4 buffer adjusted to pH=3.0 and acetonitrile (60:40 % v/v). The detection wavelength was set at 273 nm, the flow rate at 1.2 mL/min and the injection volume at 20 µL. Using this method, the retention time was approximately 7.3 minutes. The limit of detection (LOD) and quantification (LOQ) were 0.03 and 0.1 µg/mL, respectively.

2.6 Model-based analysis of *in vitro* solubility data

An experimental estimate of the naproxen pK_a was obtained by fitting the Henderson-Hasselbalch equation (Eq. 1) to the mean aqueous equilibrium solubility (S_i) values using the SIVA Toolkit® (n=6; all aqueous buffers). As intrinsic solubility (S_0), the lowest reported value in buffers was used. The pK_a

was then compared with values available in the literature to confirm the validity of the aqueous solubility parameter estimates.

$$S_i = S_0 \cdot (10^{\,pH-pKa}) \quad (1)$$

The impact of bile salt concentration ($[BS]$) and subsequent formation of micelles on the solubility of naproxen was investigated. This was done by mechanistically modelling the mean solubility values in fasted state biorelevant media (n=3), accounting also for the relative proportions of naproxen solubilized in the aqueous versus the micelle phases, using the total solubility ($S_{(BS)Tot}$) equation (Eq. 2) in SIVA Toolkit® version 3.0 (SIVA; Certara, Simcyp Division; Sheffield, UK). Estimates of the logarithm of the micelle-water partition coefficient for the neutral ($K_{m:w,unionized}$) and ionized drug ($K_{m:w,ionized}$) were obtained to quantify the micelle-mediated solubility.

$$S_{(BS)Tot} = \left([BS] \cdot \frac{S_0}{C_{H2O}} \cdot K_{m:w,unionized} + S_0 \right) + \left([BS] \cdot \frac{S_i}{C_{H2O}} \cdot K_{m:w,ionized} + S_i \right) \quad (2)$$

Where C_{H2O} stands for the concentration of water.

Estimation of the relevant parameters was performed using the Nelder-Mead algorithm and weighting by the reciprocal of the predicted values was chosen. After model verification, all obtained estimates were used as input parameters for the development of the physiologically-based pharmacokinetic model (PBPK) model (see section 2.9)

2.7 Model-based analysis of *in vitro* dissolution data

Once confidence in the estimation of solubility-related parameters was established, further model-based analysis of the *in vitro* dissolution data obtained from both the one and two-stage tests was performed within the serial dilution module of the SIVA Toolkit® (SIVA 3.0). The dissolution rate of spherical particles under sink and non-sink conditions within SIVA is described by an extension of the

diffusion layer model (DLM) developed by Wang and Flanagan. (Eq. 3) (Wang and Flanagan, 2002, 1999)

$$DR(t) = -N \cdot S_{DLM} \cdot \frac{D_{eff}}{h_{eff}(t)} \cdot 4\pi \cdot \alpha(t) \cdot \Big(\alpha(t) + h_{eff}(t)\Big) \cdot \Big(S_{surface}(t) - C_{bulk}(t)\Big) \quad (3)$$

where $DR(t)$ is the dissolution rate at time *t*; *N* is the number of particles in a given particle size bin; S_{DLM} is a lumped, empirical, correction scalar without regard to the mechanistic origin of the required correction to the DLM. The estimated S_{DLM} values obtained with SIVA can be applied to the Simcyp PBPK simulator to reflect differences between media or formulations; D_{eff} is the effective diffusion coefficient; $h_{eff}(t)$ and $\alpha(t)$ represent the thickness of the hydrodynamic boundary layer and the particle radius at time *t* respectively; $S_{surface}(t)$ corresponds to the saturation solubility at the particle surface (which may be different to the bulk fluid solubility as discussed below); and $C_{bulk}(t)$ is the concentration of dissolved drug in bulk solution at time t.

The $h_{eff}(t)$ was calculated by the fluid dynamics sub-model, which enables the hydrodynamic conditions to be described according to local conditions and stirring rate. Fluid dynamics-based $h_{eff}(t)$ is the recommended option for describing the hydrodynamics, as it permits a more rational translation of estimated parameters such as the S_{DLM} to *in vivo* conditions, in which the hydrodynamics are usually quite different to *in vitro* experiments.

The local pH at the particle surface of ionisable drugs can significantly affect the $S_{surface}$ and consequently the dissolution rate.(K. G. Mooney et al., 1981; K.G. Mooney et al., 1981a, 1981b; Ozturk et al., 1988; Serajuddin and Jarowski, 1985; Sheng et al., 2009) Since in the *in vitro* dissolution media have a somewhat higher buffer capacity than the intestinal fluids, the self-buffering effect at the solid surface can be underestimated. For this reason, the surface pH was calculated and directly input into SIVA. The calculation of the surface pH was based on the model proposed by Mooney et al.(K.G. Mooney et al., 1981a), which assumes that dissolution is the result of both chemical reaction between

the conjugate base of the buffer species and the hydrogen cations released from the dissolving drug (in this case naproxen free acid (NPX-H)) the liquid-solid interface and the diffusion of the dissolved particles to the bulk. This model is very similar to the quasi-equilibrium model published by Ozturk et al.(Ozturk et al., 1988), a derivation of which is implemented in SIVA as the default option for surface pH calculations.

By fitting the DLM model to the observed dissolution data, accurate S_{DLM} estimates for each dissolution and two-stage test were obtained. In the case of two-stage testing, the gastric and intestinal profiles were treated separately. Under fasted state intestinal conditions, naproxen is freely soluble and therefore *in vitro* dissolution is not expected to be solubility limited. In that case, disintegration of the solid dosage form in the intestinal dissolution medium might be the rate-limiting step for the *in vitro* dissolution rate, especially in single dissolution experiments where the dosage form is directly exposed to the intestinal medium without any pre-treatment with gastric medium to account for disintegration in the stomach. In order to distinguish and model the relative impact of disintegration on the overall dissolution, the first-order disintegration option was activated in SIVA and used to obtain estimates of the first-order disintegration rate constant (k_d) for these experiments. In the case of intestinal dissolution profiles generated after two-stage testing, the first-order disintegration option was deactivated since disintegration in the stomach had been already accounted for by the dissolution in the gastric medium. For dissolution experiments of the pure drug, the disintegration time was assumed to be negligible.

Estimation of the relevant parameters was performed using the Nelder-Mead algorithm and equal weighting was applied. The various estimated S_{DLM} and k_d values were implemented in the Simcyp® Simulator (V18.1; Certara, Sheffield, UK) to simulate various *in vivo* dissolution scenarios for the formulations under study and to generate *in vitro-in vivo* extrapolation relationships. These are necessary to predict the formulation or pure drug *in vivo* performance using PBPK modelling.

2.8 *In vivo* studies

Seven clinical trials published in the open literature were used in support of the development and verification of the PBPK model for naproxen. Six studies were performed after oral administration of single-dose of naproxen or its sodium salt at different dose levels in the fasted state. Data after intravenous administration were obtained from Runkel et al.(Runkel et al., 1973, 1972a, 1972b)

The results of bioavailability studies for the Naprosyn® formulation were published by Charles and Mogg(Charles and Mogg, 1994) and by Zhou et al.(Zhou et al., 1998) In the study by Charles and Mogg, sixteen Caucasian (12.5% females) healthy subjects with mean (SD) age of 22.1 (4.4) years old received one 500 mg Naprosyn® tablet with 100 mL water at 8:00 a.m. after an overnight fast. All individuals were within 20% of their ideal body weight for height and gender with a mean (SD) weight and height of 67.6 (8.3) kg and 175.7 (9.0) cm, respectively. In the study by Zhou et al., ten Chinese healthy male volunteers (with age and body weight ranging from 19-38 year and 51-74 kg respectively) received two 250 mg Naprosyn® tablets with 200 mL water at 8 a.m. after an overnight fast.

Regarding the Anaprox® formulation, a bioavailability study by Haberer et al.(Haberer et al., 2010) and a bioequivalence (BE) study by Setiawati et al.(Setiawati et al., 2009) have been reported in the literature. Using the same study design (two-treatments protocol), Haberer et al. tested the bioavailability of a tablet of 550 mg Anaprox® as well as of 500 mg of naproxen sodium, with the intention of incorporating this dose in a fixed dose combination tablet with sumatriptan. A tablet of 550 mg Anaprox® (treatment A) and of 500 mg of naproxen sodium (treatment B) were administered after an overnight fast to 8 and 16 healthy non-smoker volunteers, respectively. The proportion of females in the study was 63% and subjects had a mean (SD) age of 44.3 (8.5) years and a mean body weight of 71.44 (12.3) kilograms. In the study by Setiawati et al., twenty-six healthy volunteers (15% females), aged 19 to 46 years and with body mass index (BMI) 18-23, were administered a tablet

containing 550 mg naproxen sodium with 200 mL of water in a sitting position at 07:00 a.m. after an overnight fast.

To investigate the bioavailability of naproxen free acid, Rao et al. administered 500 mg of pure drug powder filled in hard capsules together with a glass of water to twelve Indian healthy male volunteers, aged between 18 and 22 years, who had fasted overnight.(Rao et al., 1993) In all studies, no concomitant administration of any other drugs was permitted for at least 1 week before the study and food was withheld until 3 hours post-dose.

All available demographic data from the aforementioned clinical studies were used to simulate the clinical trials and are summarized in Table 2. Since no pharmacokinetic differences due to race have been identified to date, all individuals were treated the same in terms of ethnicity for modeling purposes.

Table 2: Mean (SD) demographic data of in vivo studies used for the development and verification of the PBPK model. (HV= healthy volunteers)

2.9 Development of the middle-out PBPK model and selection of *in silico* input parameters

PBPK modeling and simulations were performed using the Simcyp® Simulator (V18.1; Certara, Sheffield, UK). The naproxen PBPK model was developed by implementing a stepwise sequential modeling strategy, in line with previously published literature and the regulatory guidelines.(European Medicines Agency (EMA), 2018b; Ke et al., 2016; Kuepfer et al., 2016; Shebley et al., 2018; U.S.FDA Center for Drug Evaluation and Research (CDER), 2018b; Zhao et al., 2012) Initially, an intravenous (IV)

model was set up and, after optimizing the distribution/elimination parameters, it was adapted to mechanistically describe oral absorption. The compound file was also informed with physicochemical parameters including molecular weight (MW), octanol:water partition coefficient ($logP_{o:w}$), fraction unbound in plasma (f_u) and blood to plasma ratio (B:P) obtained from the literature.(Bergström et al., 2014; Brown et al., 2007; Davies and Anderson, 1997; Lin et al., 1987; Paixão et al., 2012; Pérez et al., 2004; Zhao et al., 2001)

2.9.1 Intravenous (IV) model

Since the volume of distribution reported in the literature for naproxen usually lies between 0.05-0.2 L/kg (similar to the plasma water volume),(Awni et al., 1995; Franssen et al., 1986; Gøtzsche et al., 1988; Niazi et al., 1996; Upton et al., 1984; Van den Ouweland et al., 1988; Vree et al., 1993) the minimal PBPK (mPBPK) with a single adjusting compartment (SAC) was chosen as the distribution model. The mPBPK is a "lumped" PBPK model in which the SAC represents all tissues excluding liver and portal vein. Use of the SAC requires prior fitting to observed clinical data using the Simcyp® parameter estimation (PE) module. Implementing a "middle-out" strategy, the post-absorptive variables, i.e. the parameter values for volume of distribution at steady-state (V_{ss}), apparent SAC volume (V_{sac}), inter-compartmental (Q_{sac}) and *in vivo* IV clearance (CL_{IV}) were estimated using the PE module after simultaneous fitting of the mPBPK model to the observed intravenous data.(Runkel et al., 1973, 1972a, 1972b) The estimation was weighted by the number of individuals in the reported study and the resulting parameters were then compared with values reported in the literature.

2.9.2 p.o. (oral) model

For mechanistic absorption modeling the advanced dissolution absorption and metabolism (ADAM) model,(Jamei et al., 2009; S. Darwich et al., 2010) in which the gastrointestinal tract (GIT) is divided into 9 anatomically distinct segments starting from stomach through small intestine to the colon, was used. It was assumed that no drug absorption in the stomach occurred. The effective permeability ($P_{eff,man}$) value in humans was obtained from the literature,(Lennernas et al., 1995) whereas for S_0, $logK_{m:w,unionized}$, $logK_{m:w,ionized}$ the estimates from model-based analysis of the *in vitro* solubility data were implemented (see section 2.7). Default settings of the software for luminal blood flow, fluid volume, bile salt content, segmental pH, metabolic activity and small intestinal residence time were used. The mean gastric emptying time (GET) in the fasted state was set to 0.25 h (matching the built-in 'segregated transit time' model value instead of the default value of 0.4 h used in the 'global' transit time model), as suggested by human clinical data and several authors.(Cristofoletti et al., 2016; Hens et al., 2014; Paixão et al., 2018; Psachoulias et al., 2011) All relevant input parameters for the development of the PBPK models and simulations are summarized in Table 3.

Table 3: Input parameters for naproxen PBPK model development and simulations

2.10 Verification of PBPK model and Clinical Trial simulations

The performance of the developed PBPK model was verified by simulation of several clinical studies after oral administration and by comparison with the mean observed pharmacokinetic profiles already available in the literature.(Charles and Mogg, 1994; Haberer et al., 2010; Rao et al., 1993; Setiawati et al., 2009; Zhou et al., 1998) Virtual populations were selected to closely match the enrolled individuals in the respective *in vivo* clinical trials with respect to sample size, ethnicity, gender ratio, and age and weight range. Reported volumes of concomitant liquid intake, dosage form type and sampling schedule were also included in the study design.

Using an *in vitro-in vivo* extrapolation (IVIVE) approach, the various DLM scalar estimates, (see sections 2.7, 3.5) obtained by model-based analysis of the *in vitro* dissolution data with the diffusion layer model were input to best capture different *in vivo* dissolution scenarios. Further, to investigate the effect of *in vivo* dissolution of multiple formulations and under various conditions on the overall *in vivo* performance, the same DLM scalar estimates from *in vitro* dissolution data for each case were implemented to simulate the aforementioned clinical studies. Every *in vivo* dissolution scenario was evaluated by simulating of 10 trials, each with 10 subjects each (Σ=100). All virtual clinical trials were matched in terms of demographic data (e.g. gender ratio, age & weight range) as closely as possible to the reported studies.

2.11 Parameter Sensitivity Analysis (PSA)

Once confidence in the PBPK model performance was established, parameter sensitivity analysis (PSA) was conducted to identify the absorption rate limiting steps and their impact on *in vivo* performance (e.g., C_{max}, t_{max}, AUC). Variation of one or two parameters at a time over a physiologically realistic range of values was applied for gastric emptying time (GET) and the DLM scalar.

2.12 Virtual Bioequivalence (VBE) Trials

The virtual bioequivalence (VBE) trials were designed as fully replicated, two-sequence, two-treatment, two-period, crossover studies. In virtual BE studies between the hypothetical test and reference formulations, PK profiles for a total of 120 healthy adult volunteers (12 subjects in each of 10 trials) for each treatment were generated. The existing default coefficients of variation (%CV) - i.e., between subject (BS) variability of the physiological parameters stored in the Simcyp® simulator database for the North European Caucasian healthy adult volunteers' population were applied for each

parameter. As an integral part of within-subject (WS) variability, inter-occasion variability (IOV) significantly contributes to the overall population variability and therefore it should be accounted for by the PBPK models. To model IOV, a CV of 30% was set, according to the literature and unpublished data from C. Reppas.(Fruehauf et al., 2007; Grimm et al., 2018; Lartigue et al., 1994; Petring and Flachs, 1990) IOV was added through the VBE module (V1.0) of Simcyp® simulator to the mean GET, pH of fasted stomach, pH and bile salts concentration of fasted duodenum, jejunum I and II segments and mechanistically propagated in the simulations. The IOV was intentionally set to the somewhat exaggerated value of 30% for all the relevant parameters to further challenge the establishment of bioequivalence. In each trial, a pre-specified number of randomly simulated individuals (n=12) were generated for each formulation (reference and test). The relevant PK metrics (C_{max}, t_{max}, AUC) for each subject were calculated. The VBE trials were interpreted as crossover studies and average BE (ABE) was assessed using Phoenix® WinNonlin (v8.1; Certara; Princeton, NJ, USA) for each relevant PK metric. In a best-and worst-case scenario the hypothetical reference and test formulations were assumed to have *in vivo* dissolution in the virtual individuals corresponding to the highest and lowest estimated DLM scalar value, respectively, resulting from the model-based analysis of the *in vitro* dissolution data.

2.13 Data Analysis and Model Diagnostics

The solubility and dissolution data are presented as the arithmetic mean with standard deviations. Model-based analysis of the *in vitro* data in SIVA® Toolkit was performed with either the Nelder Mead or the hybrid algorithm (genetic algorithm coupled to Nelder Mead) with a 5th order Runge-Kutta or Livermore solver. Different weighting schemes were tested and the goodness of fit was assessed by the Akaike (AIC, AICc) and Bayesian (BIC) information criteria as well as the coefficient of determination (R squared). All PK profiles obtained from the literature were digitalized with the WebPlotDigitizer (version 4.1; PLOTCON; Oakland, USA). The estimation of the post-absorptive parameters within the PE module of the Simcyp® Simulator was performed with the Maximum Likelihood estimation method.

447 The prediction accuracy of the simulated plasma profiles was evaluated with the average fold error
448 (AFE) and absolute average fold error (AAFE) (see Equations 4,5).

$$AFE = 10^{\frac{1}{n}\cdot\sum \log\left(\frac{pred_t}{obs_t}\right)} \quad (4)$$

449

$$AAFE = 10^{\frac{1}{n}\cdot\sum\left|\log\left(\frac{pred_t}{obs_t}\right)\right|} \quad (5)$$

450

451

452 where n is the number of time points at which the concentration was determined and $pred_t$, obs_t are
453 the predicted and observed concentrations at a given time point t respectively. AFE deviation from
454 unity is an indication of over- ($AFE > 1$) or under-prediction ($AFE < 1$) of the observed data,
455 whereas $AAFE$ is a measure of the absolute error from the true value (or bias of the simulated profile).
456 An $AAFE \leq 2$ is considered to be a successful prediction.(Obach et al., 1997; Poulin and Theil, 2009)

457 Statistical analysis (including 95% CI) and VBE trials were performed with Simcyp® (V18.1; Certara,
458 Sheffield, UK) and Phoenix® WinNonlin (v8.1; Certara; Princeton, NJ, USA). Data post-processing and
459 plotting were performed with MATLAB® 2018a (Mathworks Inc.; Natick, MA, USA) and R® (version
460 3.5.1).

461

3 Results

3.1 *In vitro* solubility

3.1.1 Aqueous Buffers

Table 4 summarizes the equilibrium solubility values in various aqueous media of different pH. In the case of the free acid, the final pH_{bulk} differed significantly from the initial pH values due to the self-buffering effect. This behavior was not observed for the sodium salt, where the pH difference was equal or less to 0.1 pH unit. The higher solubility of the sodium salt compared to the free acid, especially in the intestinal pH media, is attributed to the difference in the final pH measured, keeping in mind that in this pH range the solubility increases exponentially with pH increase. Since naproxen is a weakly acidic compound, its pH-solubility profile is described by two regions: a) $pH < pH_{max}$, where the excess solid phase in equilibrium with the saturated solution consists of the unionized form and b) $pH > pH_{max}$, where the equilibrium species are exclusively in the ionized form.(Avdeef, 2007) Hence, unless self-association of solute molecules occurs, identical pH-solubility profiles at equilibrium are expected regardless of the starting material (free acid or salt), as shown in Figure 1. The experimental values were plotted as a pH-solubility profile and compared to values reported in the literature, showing excellent agreement (Figure 1).(Avdeef, 2007; Avdeef and Berger, 2000; Chowhan, 1978)

Table 4: Mean (± SD) equilibrium solubility in aqueous media at 37°C for 24h (Uniprep® method).

Figure 1: Naproxen (squares) and naproxen sodium (triangles) experimental mean equilibrium solubility values (24 h at 37°C) plotted against respective literature values (24 h at 25°C) in a pH-solubility profile. The in vitro solubility experiments were performed with the Uniprep® method described in section 2.2. The experimental results are in agreement with the literature values (24 h at 25°C). The literature values were obtained from Avdeef et al. (Ref. 75); Chowhan et al. (Ref. 77)

3.1.2 Biorelevant media

The solubility was additionally investigated in selected Level II fasted and fed state biorelevant media (see Table 5).(Markopoulos et al., 2015) Similar to the solubility of the free acid in phosphate buffers, a considerable decrease in the final pH_{bulk} was observed in fasted state biorelevant media. In fact, the reduction is even more pronounced in the fasted state biorelevant media due to their lower buffer capacity (5.6 mmol/L/ΔpH in FaSSIF V3 *versus* 18.5 mmol/L/ΔpH in European Pharmacopoeia phosphate buffers).(Fuchs et al., 2015) Comparison of solubilities in compendial with those in biorelevant media shows that micelle-mediated solubilization has a substantial impact on the overall solubility of naproxen. Particularly in FaSSIF V1 Level II, the solubility of both free acid and sodium salt was increased by 25.8% and 51.8%, respectively, when compared to phosphate buffer (pH=6.5). Likewise, in media simulating the fed state, such as FeSSIF V1 Level II, a 2.4-fold increase in the solubility of the free acid and a 2.1-fold increase for the salt form were observed, in comparison to the respective medium without surfactants.

Table 5: Mean (± SD) equilibrium solubility in fasted and fed state biorelevant media at 37°C for 24h (Uniprep® method).

3.2 Modeling of *in vitro* solubility

Table 6 summarizes the parameter estimates (95% CI) obtained by model-based analysis of the *in vitro* solubility data in compendial and biorelevant media, as described in section 2.6. The pK_a was determined to be 4.43, which agrees with values reported in the literature (4.15-4.5). (Avdeef, 2007; Chowhan, 1978; Davies and Anderson, 1997; McNamara and Amidon, 1986; Sheng et al., 2009) By estimating the micelle-water partition coefficients for both neutral and ionized species using the biorelevant solubilities, we were able to quantify the effect of physiologically relevant surfactants on the overall solubility of naproxen. These values were utilized within the Simcyp® Simulator to simulate the luminal conditions and the *in vivo* dissolution behavior, accounting at the same time for any inter-subject variability regarding bile salt-mediated solubilization in the virtual population. Therefore, implementation of $logK_{m:w}$ neutral and ion in the PBPK model allowed for mechanistic prediction of the *in vivo* luminal dissolution, which would not be possible if only mean solubility values had been used.

Table 6: Parameter estimates (95% CI) resulting from the model-based analysis of in vitro solubility data in aqueous as well as biorelevant media. The pka was estimated from the aqueous solubility values, whereas for the micelle-water partition coefficients ($logK_{m:w}$ neutral, ion) estimation, biorelevant solubilities were used. The accuracy of the predictions was evaluated with the R squared.

3.3 *In vitro* dissolution tests

3.3.1 Active Pharmaceutical Ingredient (API) powder

Mean percentage dissolved (± SD) over time in compendial and fasted state biorelevant media for the pure API of naproxen and its sodium salt are presented in Figure 2 and Figure 3, respectively. All dissolution experiments were performed as described in section 2.3.

For the free acid, dissolution in FaSSIF V3 Level II and in Ph. Eur. phosphate buffer pH=6.8 was very rapid (>85% within 5 minutes in FaSSIF V3) and rapid (>85% within 30 minutes in phosphate buffer). On the other hand, the dissolution in FaSSIF V3 Level I (i.e. without bile components) was much slower with 85% dissolved reached only after 60 minutes. The observed differences in *in vitro* dissolution behavior is attributed to differences in buffer capacity (FaSSIF V3 Level I and II vs. phosphate buffer) and solubilization capacity (FaSSIF V3 Level II vs. Level I) of the tested media, whereas the difference of 0.1 pH units between the initial pH of Ph. Eur. phosphate buffer pH=6.8 and FaSSIF V3 is assumed to have a negligible effect.

Especially since dissolution was under non-sink conditions in this series of experiments, the dissolution rate in FaSSIF V3 Level I was significantly slower, due to its low buffer capacity (5.6 mmol/L/ΔpH), than in the compendial phosphate buffer (13.5 vs. 50 mM phosphate buffer). At higher total phosphate buffer concentration, i.e. in the compendial medium, the bulk (pH_{bulk}) rather than the surface pH (pH_0) drives solubility and dissolution. By contrast, in the low buffer capacity FaSSIF V3 Level I medium the surface pH seems to control the dissolution rate and as a result the final pH is significantly altered (5.95 in FaSSIF V3 Level I vs. 6.62 in Ph. Eur. phosphate buffer). The effect of buffer capacity on the overall dissolution behavior becomes much less prominent when bile salts are added to the medium, as shown in Figure 2. Furthermore, it is evident that the addition of the bile salt components in FaSSIF V3 Level II markedly enhances the dissolution rate. Although the main effect is likely through solubilization, improvements in wetting may have also contributed to the higher dissolution rate in the Level II medium.

For the sodium salt, these trends were not observed and dissolution was almost instantaneous (85% dissolved by the first sampling time at 2.5 min) in all tested media. This is attributed to the higher solubility as well as higher surface pH generated by the sodium salt of naproxen.

Figure 2: In vitro dissolution (mean ± SD) of 500 mg naproxen free acid API powder in Ph. Eur. phosphate buffer (pH=6.8), Level I and II FaSSIF V3. USP paddle apparatus at 75 rpm and 500 mL of dissolution medium at 37°C were used in all experiments. The experiments were performed in triplicate. Horizontal dashed red line represents 85% dissolved. Most standard deviation bars lie within the symbols.

Figure 3: In vitro dissolution (mean ± SD) of 550 mg naproxen sodium API powder in Ph. Eur. phosphate buffer (pH=6.8), FaSSIF V3 Levels I and II. USP paddle apparatus at 75 rpm and 500 mL of dissolution medium at 37°C were used in all experiments. The experiments were performed in triplicate. Horizontal dashed red line represents 85% dissolved. Most standard deviation bars lie within the symbols.

3.3.2 Formulations

The dissolution profiles in FaSSIF V3 Levels I and II along with the results for the "intestinal" part of the two-stage testing are presented for Naprosyn® and Anaprox® in Figure 4 and Figure 5, respectively. In all cases, and for both formulations, dissolution was very rapid under conditions simulating the upper small intestine, with 85% dissolved in less than 15 min. Interestingly, a mismatch between the dissolution results of the APIs and dosage forms was observed. For instance, dissolution of the free acid form of the API was much faster from the dosage form (Naprosyn®) than from the pure API in FaSSIF V3 Level I. However, the dissolution of naproxen free acid from Naprosyn® in FaSSIF V3 Level II was slightly slower than from the pure API. Furthermore, although dissolution of sodium salt API was virtually instantaneous in all media (85% dissolved within 2.5 min), 85% dissolution was reached only after 15 minutes during release from Anaprox®.

These findings suggested that the dissolution of the tablets under intestinal conditions was delayed due to slow disintegration, especially in the case of the sodium salt formulation. In order to account for disintegration in the stomach prior to exposure to the intestinal media, two-stage dissolution tests were subsequently performed, as described in section 2.4. Since the amount dissolved under gastric conditions was less than 2% in all cases (see Figure 6), only the "intestinal" profiles of the 2-stage tests are plotted and directly compared with the conventional dissolution profiles (Figure 4 and Figure 5). Pre-treatment in gastric media accelerated the dissolution rate (85% dissolved reached 5 min earlier) of the API from both the Naprosyn® formulation of the free acid (Figure 4) and the Anaprox® formulation of the sodium salt form (Figure 5). Although in all cases dissolution would be considered very rapid, the disintegration effect was more prominent for Anaprox®, as shown also in Figure 6. A model-based analysis of the anticipated in vitro dissolution differences is presented in section 3.4.

Figure 4: In vitro dissolution (mean ± SD) of Naprosyn® 500 mg in FaSSIF V3 Levels I and II (solid lines, filled squares and circles respectively). The intestinal profiles in FaSSIF V3 Levels I and II (after the pre-treatment with FaSSGF Levels I and III respectively) during two-stage test are also depicted (dotted lines, empty squares and circles, respectively). USP paddle apparatus at 75 rpm and 500 mL of dissolution medium at 37°C were used in all experiments. The experiments were performed in triplicate. Horizontal dashed red line represents the 85% dissolved. Most standard deviation bars lie within the symbols

Figure 5: In vitro dissolution (mean ± SD) of Anaprox® 550 mg in FaSSIF V3 Levels I and II (solid lines, filled squares and circles respectively). The intestinal profiles in FaSSIF V3 Levels I and II (after the pre-treatment with FaSSGF Levels I and III respectively) during two-stage test are also depicted (dotted lines, empty squares and circles, respectively). USP paddle apparatus at 75 rpm and 500 mL of dissolution medium at 37°C were used in all experiments. The experiments were performed in triplicate. Horizontal dashed red line represents the 85% dissolved. Most standard deviation bars lie within the symbols

Figure 6: In vitro dissolution (mean ± SD) of Naprosyn® 500 mg (solid lines) and Anaprox® 550 mg (dashed lines) in FaSSGF Levels I and III (filled circles and squares, respectively). USP paddle apparatus at 75 rpm and 250 mL of dissolution medium at 37°C were used in all experiments. The experiments were performed in triplicate. Horizontal dashed red line represents the 85% dissolved. Most standard deviation bars lie within the symbols.

3.4 Modeling of *in vitro* dissolution

Table 7 and Table 8 summarize the estimated DLM scalar values (95% CI) obtained by model-based analysis of the intestinal *in vitro* dissolution profiles using the SIVA Toolkit®. Each naproxen form (i.e. pure API and formulations of each of the free acid and sodium salt) was evaluated separately. The goodness of fit was visually inspected with residuals plots and assessed with the coefficient of determination (R^2). As shown in Table 8, the first-order disintegration model without time-lag was applied only to those experiments where the formulations were not pre-exposed to gastric medium. Matching between two-stage and single dissolution, combined with the disintegration model, DLM estimates were obtained. These results indicate that the effect of disintegration can be properly accounted for using the methodology applied.

The slowest and fastest dissolution rate of the acid form of the API observed in FaSSIF V3 Levels I and II, respectively, resulted in the lowest (0.0022) and highest (0.0810) estimated DLM values. Due to the virtually instantaneous dissolution of the sodium salt API in all media, the default DLM value of 1, without estimation, was utilized for the salt form (Table 7). The predicted dissolution profiles were in excellent agreement with the experimental profiles ($R^2 > 0.96$).

Table 7 : Estimated DLM scalar values (95% CI) obtained from model-based analysis of in vitro dissolution in various media of naproxen free acid and sodium salt pure API powder. The goodness of fit between predicted and observed dissolution profiles was evaluated with the R squared (R^2).

Table 8: Estimated DLM scalar and first-order disintegration rate constant (k_d) values (95% CI) obtained from model-based analysis of in vitro dissolution in various media of naproxen free acid (Naprosyn®) and sodium salt (Anaprox®) formulation. In case of dissolution without pre-treatment in a gastric medium, a first-order disintegration model was included. The goodness of fit between predicted and observed dissolution profiles was evaluated with the R squared (R^2).

3.5 PBPK model verification & clinical trial simulations

The PBPK model of naproxen was developed and verified as described in sections 2.9 and 2.10, respectively. Post-absorptive parameters (CL, V_{ss}, V_{sac}, Q_{sac}) were estimated from intravenous data, whereas for dissolution-absorption the Diffusion layer model-ADAM was used. Different *in vivo* dissolution scenarios were simulated according to the DLM scalar values obtained by model-based analysis of *in vitro* biorelevant dissolution profiles of the tested naproxen forms. The simulated profiles were compared against observed data from human *in vivo* PK studies (see section 2.8). The generated virtual population closely matched the individuals enrolled in the respective *in vivo* studies in terms of ethnicity, gender ratio, and age and weight range. Volumes of concomitant liquid intake, dosage form type and sampling schedule were also taken into account for the virtual study design wherever available (see details in section 2.10).

Table 9 summarizes all the simulations (10 trials by 10 individuals) performed for each *in vivo* dissolution scenario and the resulting mean *in silico* population pharmacokinetic (popPBPK) parameters for the virtual healthy adult population. Regardless of the anticipated differences in *in vivo* dissolution, as reflected by the various estimated DLM values, these results suggest that mean AUC remains almost constant, while more pronounced variations in C_{max} and especially in t_{max} are observed.

649 Direct comparisons of the mean *in silico* and *in vivo* pharmacokinetic parameters show very good
650 agreement between simulated and observed data (Table 9 and Table 10). In all cases, the average (AFE)
651 and absolute average fold error (AAFE) lay between 0.90-1.16 and 1.07-1.04, reflecting successful PBPK
652 model performance and excellent predictions of the observed plasma profiles.

653 Figure 7 illustrates the mean simulated naproxen plasma-concentration time profiles and the 5th and
654 95th percentiles of the virtual population for the two extreme DLM estimated values; i.e.,
655 DLM_{min}=0.0022 and DLM_{max} = 1. Note that these DLM values were extracted from the dissolution of
656 the free acid and salt pure API forms, not the formulations, and were intentionally chosen as such in
657 order to evaluate *in vivo* performance differences (if any) that could be detected under these extreme
658 scenarios. As can be observed, the C_{max} of the simulated plasma profile corresponding to
659 administration of the very slowly dissolving hypothetical formulation was only slightly lower than the
660 one resulting from the very fast dissolving hypothetical formulation. On the other hand, tmax was
661 significantly prolonged. Interestingly, regardless of whether the worst or best case scenario was
662 applied, the dissolution profiles predicted the observed range of PK profiles reasonably well (see also
663 AFE and AAFE values).

664 In order to further explore the impact of key parameters on the simulated plasma profiles, one-at-a-
665 time parameter sensitivity analysis (PSA) on the DLM scalar and GET in the fasted state was performed.
666 GET and DLM were allowed to range from 0.1 to 2 hours and 0.001 to 0.1, respectively, while all other
667 parameters in the model were kept constant. Figure 8 and Figure 9 show the mean simulated plasma
668 profiles of a representative individual of the virtual population for various DLM and GET values,
669 respectively. Figure 8 shows that over a 100-fold range of DLM values only slight or almost no
670 differences in C_{max} (69.7-74.0 mg/L) or AUC (1175-1177 mg/L · h) are observed. T_{max} (1.40-2.65 h) seems
671 to be more sensitive to *in vivo* dissolution changes (as reflected in the S_{DLM} values) than the other PK
672 parameters. Figure 9 clearly demonstrates that variation in GET markedly affects C_{max} (52.2-75.5 mg/L)
673 and t_{max} (1.09-4.00 h), whereas AUC (1172-1180 mg/L · h) is not impacted.

As one would anticipate, PSA on dissolution rate in the stomach revealed no changes in the simulated C_{max}, t_{max} and AUC (data not shown), since poorly soluble weakly acidic compounds like naproxen barely dissolve in the fasted state gastric environment (see also Figure 6).

Table 9: Mean in silico population pharmacokinetic (popPBPK) parameters of naproxen simulated plasma-concentration-time profiles under all tested in vivo dissolution inputs (DLM scalar values) as obtained from model-based analysis of the in vitro data (see formulation and dissolution medium).

Table 10: Mean (SD) pharmacokinetic parameters of naproxen in vivo studies ([a] Median value).

Figure 7: Population mean simulated naproxen plasma concentration-time profiles and the 5th and 95th percentiles for the two extremes of the estimated S_{DLM} values: (a) S_{DLM}=1 (green and grey solid lines, respectively) and (b) DLM=0.0022 (blue and light grey dashed lines, respectively). In a worst/ best case virtual bioequivalence scenario of simulated healthy adult populations (a) was treated as the reference, whereas (b) as the test formulation. Observed clinical data from Charles & Mogg (circles), Zhout et al. (squares), Haberer et al. (a) (diamonds), Setiawati et al. (triangles), Rao et al. (crosses) and Haberer et al. (b) (asterisks) are overlaid for verification of the PBPK model performance and comparisons. Simulations run for 72 h, but to enable better comparison only the first 24 hours are plotted.

Figure 8: Sensitivity analysis of naproxen simulated plasma concentration-time profiles of population representative individual on DLM scalar values ranging from 0.001 (blue solid line) to 0.1 (dashed line). The values of all other parameters were kept constant (GET=0.25 h). Observed clinical data from Charles & Mogg (circles), Zhout et al. (squares), Haberer et al. (a) (diamonds), Setiawati et al. (triangles), Rao et al. (crosses) and Haberer et al. (b) (asterisks) are overlaid for comparisons. Simulations run for 72 h, but to enable better comparison only the first 24 hours are plotted.

Figure 9: Sensitivity analysis of naproxen simulated plasma concentration-time profiles of population representative individual on GET values in fasted state ranging from 0.1 (blue solid line) to 2 hours (dash double dotted line). The values of all other parameters were kept constant (DLM= 1). Observed clinical data from Charles & Mogg (circles), Zhout et al. (squares), Haberer et al. (a) (diamonds), Setiawati et al. (triangles), Rao et al. (crosses) and Haberer et al. (b) (asterisks) are overlaid for comparisons. Simulations run for 72 h, but to enable better comparison only the first 24 hours are plotted.

688

689 3.6 Virtual Bioequivalence

690

691 Multiple non-replicated, two-sequence, two-treatment, two-period, cross-over virtual bioequivalence
692 trials (n=10) with 12 individuals per trial were conducted. In a worst/ best case scenario, two
693 hypothetical naproxen formulations with extremely different *in vivo* dissolution rates were tested with
694 the aim of designing a clinically relevant safe space. The reference (R) was assumed to have a DLM
695 scalar value of 1, corresponding to the instantaneous dissolution of naproxen sodium API powder,
696 while the test (T) formulation was assigned the value of 0.0022, corresponding to the very slow
697 dissolution of naproxen free acid API powder in FaSSIF V3 Level I (Table 11).

698 Figure 10 presents the results of virtual bioequivalence trials for C_{max}, AUC calculated up to the last
699 simulated time point (AUC_{tlast}) and extrapolated to infinity (AUC_{inf}). Bioequivalence with regard to t_{max}
700 was also investigated. In all trials, C_{max}, AUC_{tlast}, AUC_{inf} met the average bioequivalence criteria (80-
701 125%) with confidence intervals (CI) narrowly distributed around unity, especially for AUC. However,
702 in terms of t_{max} bioequivalence failed in all 10 trials and most CI were far beyond the bioequivalence
703 limits. These findings suggest that naproxen formulations which reach 85% dissolved in media
704 simulating the healthy human upper small intestine within 90 minutes or less are expected to be
705 bioequivalent. These borders correspond to the dissolution "safe space" and can be used to set
706 clinically relevant dissolution specifications to minimize the risk of bioequivalence failure.

Table 11: Mean in silico population pharmacokinetic (popPBPK) parameters of naproxen virtual clinical trials for the hypothetical reference and test formulations prior to bioequivalence assessment.

Figure 10: Average virtual bioequivalence results (% Geometric mean T/R ratio) of 10 trials with 12 simulated individuals in each trial. Intra-subject variability of 30% was arbitrarily chosen and added through Simcyp ® (V18.1; Certara, Sheffield, UK) VBE module (V1.0) to the mean GET, pH of fasted stomach, pH and bile salts concentration of fasted duodenum, jejunum I and II. The 80-125% bioequivalence limits (red dashed lines) and the area of acceptance (light green shaded area) are shown for each tested PK parameter: (A) C_{max}, (B) AUC_{tlast} (AUC calculated up to the last simulated time point), (C) AUC_{inf} (AUC extrapolated to infinity) and (D) t_{max}. Error bars represent the 90% confidence intervals, which in subplots (B) and (C) lie within the symbols.

Figure 11: Dissolution safe space for anticipated bioequivalence to naproxen products. The light green shaded area delimits the safe space area in which bioequivalence (with respect to C_{max} and AUC) was established between the very slow (red solid line & squares) and the fast (blue solid line & circles) dissolution profiles. Additional typical dissolution profiles are co-plotted (n=3). The horizontal red dashed line represents 85% dissolved.

4 Discussion

The present study proposes a workflow and highlights the key role of mechanistic absorption and population-based PBPK modeling to establish virtual bioequivalence and set clinically relevant dissolution specifications by combining *in vitro*, *in vivo* and *in silico* methods.

In the naproxen case example, starting from *in vitro* solubility and dissolution data, an approach of stepwise sequential estimation/confirmation of biopharmaceutical parameters was followed,(Pathak et al., 2019) before applying them to the PBPK model. *In vitro* dissolution profiles in conventional and biorelevant media were translated to different *in vivo* dissolution scenarios by implementing an *in vitro-in vivo*-extrapolation (IVIVE) strategy. The healthy adult PBPK model for naproxen was developed by optimizing post-absorptive parameters from intravenous in vivo data which was then coupled with the ADAM model for mechanistic oral absorption modelling. The verification of the PBPK model was based on its ability to predict the observed plasma PK profiles after oral administration of naproxen in several *in vivo* studies and its performance under multiple *in vivo* dissolution scenarios was assessed.

Simulations of the clinical studies in conjunction with sensitivity analysis on the DLM scalar and gastric emptying time revealed that C_{max} and AUC are rather insensitive to dissolution changes, but that C_{max} is considerably affected by variations in gastric emptying time. However, changes in either the S_{DLM} or gastric emptying markedly altered t_{max}. These results indicate that the absorption and thus the *in vivo* performance of naproxen formulations seem to be governed by gastric emptying, but is not dissolution-limited. This is supported by the (refined) developability classification system (DCS/ rDCS),(Butler and Dressman, 2010; Rosenberger et al., 2019) according to which naproxen would more appropriately be classified as rDCS/ DCS I, and is in excellent agreement with the study of Charles and Mogg(Charles and Mogg, 1994), which concluded that two naproxen products (tablet and caplet) with

very dissimilar *in vitro* dissolution behavior were bioequivalent. Furthermore, a DLM scalar range from 0.0022 to 1 translated to an increase in C_{max} only by 1.06 and 1.75 times earlier t_{max}, assuming the default in Simcyp particle radius of 10 µm. The AUC remained unchanged. In this case, the insensitivity of PK metrics to the dissolution rate was attributed both to the absence of saturable first pass extraction and the relatively long half-life ($t_{1/2}$≈20 h) of the drug.

Once enough confidence with the performance of the PBPK model was achieved, several VBE trials simulating a worst/best case scenario were performed. A safe space and a clinically relevant dissolution specification for naproxen products was proposed based on the outcome of these virtual trials. It was demonstrated that 85% dissolved reached within 90 minutes lies comfortably within a region of dissolution performance where bioequivalence is anticipated and is not anywhere near the edge of failure for either C_{max} or AUC. On the other hand, bioequivalence in t_{max} failed in all cases. In this study, *in vitro* dissolution of unformulated free acid and sodium salt forms of naproxen were used to simulate the worst/best case BE scenario. Although this constitutes an extreme limitation, it was done intentionally to challenge the VBE result, since if the VBE were to be based solely on the dissolution of the formulations, the safe space would be biased towards an already (partly) optimized formulation range.

Virtual bioequivalence studies have been already published in the recent past(Babiskin and Zhang, 2015; Doki et al., 2017; Pathak et al., 1997; Pepin et al., 2016; Wedagedera et al., 2017; Zhang et al., 2017) However, in most of those studies the intra-subject (IIV) and inter-occasion (IOV) variability is either ignored or added directly to the PK metrics (i.e. C_{max} and AUC) as random error terms. By contrast, in the current study the intra-subject variability was added via the Simcyp® v18.1 VBE module 1.0 in several key absorption parameters, such as gastric emptying time, pH of fasted stomach, pH and bile salts concentration of fasted duodenum, jejunum I and II, and mechanistically propagated in simulations. In the context of challenging the establishment of bioequivalence, IOV was set to a somewhat exaggerated value of 30% for all parameters.

5 Conclusion

Mechanism-based absorption PBPK modeling can be considered as a promising and powerful bioequivalence risk assessment tool. This work highlights the importance of linking translational absorption modeling with population PBPK to examine VBE and set clinically relevant specifications. For naproxen, it was demonstrated that bioequivalence failure due to dissolution is unlikely for naproxen products because of the wide safe space. The example of naproxen illustrates that the impact of formulation on the *in vivo* performance is not always correlated with the *in vitro* dissolution behavior.

To the best of our knowledge, this is the first work which not only mechanistically incorporates inter-occasion variability in VBE assessment, but also propagates IOV in the simulations. Implementation of hierarchical levels of variability (BS, WS, IOV) in VBE trials is of critical importance in order to accurately describe the population variability and avoid biased, overoptimistic bioequivalence results due to underestimation of the overall variability. Even though mixed effect modelling is rare in this context, this study highlights the importance of mechanistically assigning between-subject and inter-occasion variability values which are physiologically plausible and meaningful. Using %CV values obtained from single observation in each individual within a specific population is not representative of the population BS or IOV since it comes solely from a single sample. In this case, the applied coefficient of variation is often conveniently misinterpreted as mixture of BS and IO variability. Likewise, implementation of arbitrary CV% values is inappropriate.

Moving a step further towards linking the lab to the patient, mechanistic extrapolation of in vitro data (e.g. dissolution) to the in vivo situation, as explicitly demonstrated for naproxen, is critical for the

validity and interpretation of VBE results. In the context of bioequivalence trial simulation, which is of great interest for both regulatory agencies and the pharmaceutical industry, a mechanistic IVIVE approach will be essential to enable extrapolation to specific or disease populations, given that differences in factors like GI physiology need to be taken into account. The acquisition of further clinical data (e.g., intraluminal and plasma concentrations) as well as advancement of the current biopharmaceutic tools are expected to significantly increase the reliability of virtual bioequivalence results in a variety of diseases, dosing conditions such as PPI co-administration and specific populations such as pediatric patients.

Consideration of drug-related pharmacokinetic characteristics (e.g., half-life, first pass effect, protein binding) along with PBPK modeling will assist not only to select the most appropriate dosage form and to set formulation targets, but more importantly to understand to what extent the formulation can be expected to steer the *in vivo* performance of the drug product. Further validation of the proposed approach with a range of drugs and formulations is needed to increase confidence and spread awareness of the power of mechanistic absorption modeling and PBPK in formulation design and regulation.

Bridging the gap between *in vitro*, *in vivo* and *in silico* by applying mechanistic absorption coupled with population PBPK modeling can guide model-informed formulation selection, allow for robust clinical outcome predictions, inform regulatory decision-making, permit regulatory flexibility (e.g. granting biowaivers for some BCS class II weak acids like naproxen) and potentially reduce the cost/time of product development by replacing unnecessary clinical trials.

Future work could investigate the impact of bioinequivalence in t_{max} on the onset of action and therefore the therapeutic equivalence of naproxen products. As has already been highlighted,(Cristofoletti et al., 2018; Loisios-Konstantinidis et al., 2019) a scenario is foreseen in which by combining verified PBPK with pharmacodynamic (PD) models tailored to the target population(s), release testing in the laboratory will be linked to the therapeutic outcome.

6 Acknowledgments

This work was supported by the European Union's Horizon 2020 Research and Innovation Programme under grant agreement No 674909 (PEARRL).

7 References

Avdeef, A., 2007. Solubility of sparingly-soluble ionizable drugs. Adv. Drug Deliv. Rev. 59, 568–590.

Avdeef, A., Berger, C.M., 2000. pH-Metric Solubility. 2: Correlation Between the Acid-Base Titration and formulations for use in early animal bioavailability and toxicity studies. Later in development, solubility takes on a broader. Pharm. Res. 17.

Awni, W.M., Braeckman, R.A., Cavanaugh, J.H., Locke, C.S., Linnen, P.J., Granneman, G.R., Dubé, L.M., 1995. The Pharmacokinetic and Pharmacodynamic Interactions between the 5-Lipoxygenase Inhibitor Zileuton and the Cyclo-Oxygenase Inhibitor Naproxen in Human Volunteers. Clin. Pharmacokinet. 29, 112–124.

Babiskin, A.H., Zhang, X., 2015. Application of Physiologically Based Absorption Modeling for Amphetamine Salts Drug Products in Generic Drug Evaluation. J. Pharm. Sci. 104, 3170–3182.

Bergström, C.A.S., Andersson, S.B.E., Fagerberg, J.H., Ragnarsson, G., Lindahl, A., 2014. Is the full potential of the biopharmaceutics classification system reached? Eur. J. Pharm. Sci. 57, 224–231.

Brown, H.S., Griffin, M., Houston, J.B., Li, A.P., 2007. Evaluation of cryopreserved human hepatocytes as an alternative in vitro system to microsomes for the prediction of metabolic clearance. Drug Metab. Dispos. 35, 293–301.

Butler, J.M., Dressman, J.B., 2010. The Developability Classification System: Application of Biopharmaceutics Concepts to Formulation Development. J. Pharm. Sci. 99, 4940–4954.

Charles, B.G., Mogg, G.A.G., 1994. Comparative in vitro and in vivo bioavailability of naproxen from tablet and caplet formulations. Biopharm. Drug Dispos. 15, 121–128.

Chowhan, Z.T., 1978. pH–Solubility Profiles of Organic Carboxylic Acids and Their Salts. J. Pharm. Sci.

837 67, 1257–1260.

838 Cristofoletti, R., Chiann, C., Dressman, J.B., Storpirtis, S., 2013. A comparative analysis of
839 biopharmaceutics classification system and biopharmaceutics drug disposition classification
840 system: A cross-sectional survey with 500 bioequivalence studies. J. Pharm. Sci. 102, 3136–
841 3144.

842 Cristofoletti, R., Dressman, J.B., 2016. Bridging the Gap Between In Vitro Dissolution and the Time
843 Course of Ibuprofen-Mediating Pain Relief. J. Pharm. Sci. 105, 3658–3667.

844 Cristofoletti, R., Patel, N., Dressman, J.B., 2016. Differences in Food Effects for 2 Weak Bases With
845 Similar BCS Drug-Related Properties: What Is Happening in the Intestinal Lumen? J. Pharm. Sci.
846 105, 2712–2722.

847 Cristofoletti, R., Rowland, M., Lesko, L.J., Blume, H., Rostami-Hodjegan, A., Dressman, J.B., 2018. Past,
848 Present, and Future of Bioequivalence: Improving Assessment and Extrapolation of Therapeutic
849 Equivalence for Oral Drug Products. J. Pharm. Sci. 107, 2519–2530.

850 Davies, N.M., Anderson, K.E., 1997. Clinical pharmacokinetics of naproxen. Clin. Pharmacokinet. 32,
851 268–293.

852 Dickinson, P.A., Lee, W.W., Stott, P.W., Townsend, A.I., Smart, J.P., Ghahramani, P., Hammett, T.,
853 Billett, L., Behn, S., Gibb, R.C., Abrahamsson, B., 2008. Clinical Relevance of Dissolution Testing
854 in Quality by Design. AAPS J. 10, 380–390.

855 Doki, K., Darwich, A.S., Patel, N., Rostami-Hodjegan, A., 2017. Virtual bioequivalence for achlorhydric
856 subjects: The use of PBPK modelling to assess the formulation-dependent effect of
857 achlorhydria. Eur. J. Pharm. Sci. 109, 111–120.

858 European Medicines Agency (EMA), 2018a. Committee for Medicinal Products for Human Use
859 (CHMP) Guideline on the reporting of physiologically based pharmacokinetic (PBPK) modelling

and simulation.

European Medicines Agency (EMA), 2018b. Committee for Medicinal Products for Human Use (CHMP) Guideline on the reporting of physiologically based pharmacokinetic (PBPK) modelling and simulation.

Franssen, M.J., Tan, Y., van de Putte, L.B., van Ginneken, C.A., Gribnau, F.W., 1986. Pharmacokinetics of naproxen at two dosage regimens in healthy volunteers. Int. J. Clin. Pharmacol. Ther. Toxicol. 24, 139–42.

fruehauf, h., goetze, o., steingoetter, a., kwiatek, m., boesiger, p., thumshirn, m., schwizer, w., fried, m., 2007. Intersubject and intrasubject variability of gastric volumes in response to isocaloric liquid meals in functional dyspepsia and health. Neurogastroenterol. Motil. 19, 553–561.

Fuchs, A., Leigh, M., Kloefer, B., Dressman, J.B., 2015. Advances in the design of fasted state simulating intestinal fluids: FaSSIF-V3. Eur. J. Pharm. Biopharm. 94, 229–240.

Gøtzsche, P.C., Andreasen, F., Egsmose, C., Lund, B., 1988. Steady state pharmacokinetics of naproxen in elderly rheumatics compared with young volunteers. Scand. J. Rheumatol. 17, 11–6.

Grimm, M., Koziolek, M., Kühn, J.P., Weitschies, W., 2018. Interindividual and intraindividual variability of fasted state gastric fluid volume and gastric emptying of water. Eur. J. Pharm. Biopharm. 127, 309–317.

Haberer, L.J., Walls, C.M., Lener, S.E., Taylor, D.R., McDonald, S.A., 2010. Distinct pharmacokinetic profile and safety of a fixed-dose tablet of sumatriptan and naproxen sodium for the acute treatment of migraine. Headache 50, 357–373.

Heimbach, T., Laisney, M., Samant, T., Elmeliegy, M., Wu, F., Hanna, I., Lin, W., Zhang, J., Dodd, S.,

883 Nguyen-Trung, A.-T., Tian, H., Vogg, B., Beato, S., Garad, S., Choudhury, S., Ren, X., Mueller-
884 Zsigmondy, M., Einolf, H., Umehara, K., Hourcade-Potelleret, F., He, H., n.d. PBPK Modeling and
885 Simulations of Oral Drug Absorption/Food Effect/PPI /PBIVIVC: Opportunities and Challenges
886 Dissolution and Translational Modeling Strategies Enabling Patient-Centric Product
887 Development.

888 Heimbach, T., Suarez-Sharp, S., Kakhi, M., Holmstock, N., Olivares-Morales, A., Pepin, X., Sjögren, E.,
889 Tsakalozou, E., Seo, P., Li, M., Zhang, X., Lin, H.-P., Montague, T., Mitra, A., Morris, D., Patel, N.,
890 Kesisoglou, F., 2019. Dissolution and Translational Modeling Strategies Toward Establishing an
891 In Vitro-In Vivo Link—a Workshop Summary Report. AAPS J. 21, 29.

892 Hens, B., Brouwers, J., Anneveld, B., Corsetti, M., Symillides, M., Vertzoni, M., Reppas, C., Turner,
893 D.B., Augustijns, P., 2014. Gastrointestinal transfer: In vivo evaluation and implementation in in
894 vitro and in silico predictive tools. Eur. J. Pharm. Sci. 63, 233–242.

895 Jamei, M., Turner, D., Yang, J., Neuhoff, S., Polak, S., Rostami-Hodjegan, A., Tucker, G., 2009.
896 Population-based mechanistic prediction of oral drug absorption. AAPS J. 11, 225–237.

897 Kambayashi, A., Blume, H., Dressman, J., 2013. Understanding the in vivo performance of enteric
898 coated tablets using an in vitro-in silico-in vivo approach: Case example diclofenac. Eur. J.
899 Pharm. Biopharm. 85, 1337–1347.

900 Ke, A., Barter, Z., Rowland-Yeo, K., Almond, L., 2016. Towards a Best Practice Approach in PBPK
901 Modeling: Case Example of Developing a Unified Efavirenz Model Accounting for Induction of
902 CYPs 3A4 and 2B6. CPT Pharmacometrics Syst. Pharmacol. 5, 367–376.

903 Kuepfer, L., Niederalt, C., Wendl, T., Schlender, J.-F., Willmann, S., Lippert, J., Block, M., Eissing, T.,
904 Teutonico, D., 2016. Applied Concepts in PBPK Modeling: How to Build a PBPK/PD Model. CPT
905 pharmacometrics Syst. Pharmacol. 5, 516–531.

906 Lartigue, S., Bizais, Y., Des Varannes, S.B., Murat, A., Pouliquen, B., Galmiche, J.P., 1994. Inter- and

907 intrasubject variability of solid and liquid gastric emptying parameters. A scintigraphic study in
908 healthy subjects and diabetic patients. Dig. Dis. Sci. 39, 109–15.

909 Lennernas, H., Knutson, L., Knutson, T., Lesko, L., Salmonson, T., Amidon, G.L., 1995. Human effective
910 permeability data for furosemide, hydrochlorothiazide, ketoprofen and naproxen to be used in
911 the proposed biopharmaceutical classification for IR-products. Pharm. Res. (New York) 12(9
912 SUPPL) 396.

913 Lin, J.H., Cocchetto, D.M., Duggan, D.E., 1987. Protein binding as a primary determinant of the clinical
914 pharmacokinetic properties of non-steroidal anti-inflammatory drugs. Clin. Pharmacokinet. 12,
915 402–432.

916 Loisios-Konstantinidis, I., Paraiso, R.L.M., Fotaki, N., McAllister, M., Cristofoletti, R., Dressman, J.,
917 2019. Application of the relationship between pharmacokinetics and pharmacodynamics in drug
918 development and therapeutic equivalence: a PEARRL review. J. Pharm. Pharmacol. 71, 699–723.

919 Mann, J., Dressman, J., Rosenblatt, K., Ashworth, L., Muenster, U., Frank, K., Hutchins, P., Williams, J.,
920 Klumpp, L., Wielockx, K., Berben, P., Augustijns, P., Holm, R., Hofmann, M., Patel, S., Beato, S.,
921 Ojala, K., Tomaszewska, I., Bruel, J.-L., Butler, J., 2017. Validation of Dissolution Testing with
922 Biorelevant Media: An OrBiTo Study. Mol. Pharm. 14, 4192–4201.

923 Markopoulos, C., Andreas, C.J., Vertzoni, M., Dressman, J., Reppas, C., 2015. In-vitro simulation of
924 luminal conditions for evaluation of performance of oral drug products: Choosing the
925 appropriate test media. Eur. J. Pharm. Biopharm. 93, 173–182.

926 McNamara, D.P., Amidon, G.L., 1986. Dissolution of acidic and basic compounds from the rotating
927 disk: Influence of convective diffusion and reaction. J. Pharm. Sci. 75, 858–868.

928 Mitra, A., 2019. Maximizing the Role of Physiologically Based Oral Absorption Modeling in Generic
929 Drug Development. Clin. Pharmacol. Ther. 105, 307–309.

930 Mooney, K. G., Mintun, M.A., Himmelstein, K.J., Stella, V.J., 1981. Dissolution kinetics of carboxylic
931 acids I: Effect of pH under unbuffered conditions. J. Pharm. Sci. 70, 13–22.

932 Mooney, K.G., Mintun, M.A., Himmelstein, K.J., Stella, V.J., 1981a. Dissolution Kinetics of Carboxylic
933 Acids II: Effect of Buffers. J. Pharm. Sci. 70, 22–32.

934 Mooney, K.G., Rodriguez-gaxiola, M., Mintun, M., Himmelstein, K.J., Stella, V.J., 1981b. Dissolution
935 Kinetics of Phenylbutazone. J. Pharm. Sci. 70, 1358–1365.

936 Niazi, S.K., Mahmood Alam, S., Ahmad, S.I., 1996. Dose dependent pharmacokinetics of naproxen in
937 man. Biopharm. Drug Dispos. 17, 355–361.

938 Obach, R.S., Baxter, J.G., Liston, T.E., Silber, B.M., Jones, B.C., MacIntyre, F., Rance, D.J., Wastall, P.,
939 1997. The prediction of human pharmacokinetic parameters from preclinical and in vitro
940 metabolism data. J. Pharmacol. Exp. Ther. 283, 46–58.

941 Olivares-Morales, A., Ghosh, A., Aarons, L., Rostami-Hodjegan, A., 2016. Development of a Novel
942 Simplified PBPK Absorption Model to Explain the Higher Relative Bioavailability of the OROS®
943 Formulation of Oxybutynin. AAPS J. 18, 1532–1549.

944 Ozturk, S.S., Palsson, B.O., Dressman, J.B., 1988. Dissolution of Ionizable Drugs in Buffered and
945 Unbuffered Solutions. Pharm. Res. 05, 272–282.

946 Paixão, P., Bermejo, M., Hens, B., Tsume, Y., Dickens, J., Shedden, K., Salehi, N., Koenigsknecht, M.J.,
947 Baker, J.R., Hasler, W.L., Lionberger, R., Fan, J., Wysocki, J., Wen, B., Lee, A., Frances, A.,
948 Amidon, G.E., Yu, A., Benninghoff, G., Löbenberg, R., Talattof, A., Sun, D., Amidon, G.L., 2018.
949 Gastric emptying and intestinal appearance of nonabsorbable drugs phenol red and
950 paromomycin in human subjects: A multi-compartment stomach approach. Eur. J. Pharm.
951 Biopharm. 129, 162–174.

952 Paixão, P., Gouveia, L.F., Morais, J.A.G., 2012. Prediction of the human oral bioavailability by using in

953 vitro and in silico drug related parameters in a physiologically based absorption model. Int. J.
954 Pharm. 429, 84–98.

955 Parrott, N., Hainzl, D., Scheubel, E., Krimmer, S., Boetsch, C., Guerini, E., Martin-Facklam, M., 2014.
956 Physiologically Based Absorption Modelling to Predict the Impact of Drug Properties on
957 Pharmacokinetics of Bitopertin. AAPS J. 16, 1077–1084.

958 Pathak, S.M., Patel, N., Wedagedera, J., Turner, D.B., Jamei, M., Rostami-Hodjegan, A., Limited, S.,
959 1997. Establishment of Virtual Bioequivalence Using Population-Based PBPK Modelling:
960 Application to the Setting of Dissolution Limits, AAPS J.

961 Pathak, S.M., Schaefer, K.J., Jamei, M., Turner, D.B., 2019. Biopharmaceutic IVIVE—Mechanistic
962 Modeling of Single- and Two-Phase In Vitro Experiments to Obtain Drug-Specific Parameters for
963 Incorporation Into PBPK Models. J. Pharm. Sci. 108, 1604–1618.

964 Pepin, X.J.H., Flanagan, T.R., Holt, D.J., Eidelman, A., Treacy, D., Rowlings, C.E., 2016. Justification of
965 Drug Product Dissolution Rate and Drug Substance Particle Size Specifications Based on
966 Absorption PBPK Modeling for Lesinurad Immediate Release Tablets.

967 Pérez, M.A.C., Sanz, M.B., Torres, L.R., Évalos, R.G., González, M.P., Díaz, H.G., 2004. A topological
968 sub-structural approach for predicting human intestinal absorption of drugs. Eur. J. Med. Chem.
969 39, 905–916.

970 Petring, O.U., Flachs, H., 1990. Inter- and intrasubject variability of gastric emptying in healthy
971 volunteers measured by scintigraphy and paracetamol absorption. Br. J. Clin. Pharmacol. 29,
972 703–8.

973 Poulin, P., Theil, F.-P., 2009. Development of a novel method for predicting human volume of
974 distribution at steady-state of basic drugs and comparative assessment with existing methods.
975 J. Pharm. Sci. 98, 4941–4961.

976 Psachoulias, D., Vertzoni, M., Goumas, K., Kalioras, V., Beato, S., Butler, J., Reppas, C., 2011.
977 Precipitation in and Supersaturation of Contents of the Upper Small Intestine After
978 Administration of Two Weak Bases to Fasted Adults. Pharm. Res. 28, 3145–3158.

979 Rao, B.R., Rambhau, D., Rao, V.V.S., 1993. Pharmacokinetics of Single-Dose Administration of
980 Naproxen at 1O : OO and 22 : OO Hours. Int. Soc. Chronobiol. 10, 137–142.

981 Rosenberger, J., Butler, J., Muenster, U., Dressman, J., 2019. Application of a Refined Developability
982 Classification System. J. Pharm. Sci. 108, 1090–1100.

983 Runkel, R., Chaplin, M., Boost, G., Segre, E., Forchielli, E., 1972a. Absorption, Distribution,
984 Metabolism, and Excretion of Naproxen in Various Laboratory Animals and Human Subjects. J.
985 Pharm. Sci. 61, 703–708.

986 Runkel, R., Forchielli, E., Boost, G., Chaplin, M., Hill, R., Sevelius, H., Thompson, G., Segre, E., 1973.
987 Naproxen-metabolism, excretion and comparative pharmaco kinetics. Scand J Rheumatol. 2,
988 29–36.

989 Runkel, R., Karl, K., Boost, G., Sevilius, H., Forchielli, E., HILL, R., MAGOUN, R., SZAKACS, J.B., SEGRE,
990 E., 1972b. Naproxen Oral Absorption Characteristics. Chem. Pharm. Bull. (Tokyo). 20, 1457–
991 1466.

992 S. Darwich, A., Neuhoff, S., Jamei, M., Rostami-Hodjegan, A., 2010. Interplay of Metabolism and
993 Transport in Determining Oral Drug Absorption and Gut Wall Metabolism: A Simulation
994 Assessment Using the “Advanced Dissolution, Absorption, Metabolism (ADAM)” Model. Curr.
995 Drug Metab. 11, 716–729.

996 Selen, A., Dickinson, P.A., Müllertz, A., Crison, J.R., Mistry, H.B., Cruañes, M.T., Martinez, M.N.,
997 Lennernäs, H., Wigal, T.L., Swinney, D.C., Polli, J.E., Serajuddin, A.T.M., Cook, J.A., Dressman,
998 J.B., 2014. The biopharmaceutics risk assessment roadmap for optimizing clinical drug product
999 performance. J. Pharm. Sci. 103, 3377–3397.

1000 Serajuddin, A.T.M., Jarowski, C., 1985. Effect of diffusion layer pH and solubility on the dissolution
1001 rate of pharmaceutical bases and their hydrochloride salts. I: Phenazopyridine. J. Pharm. Sci. 74,
1002 142.

1003 Setiawati, E., Deniati, S., Yunaidi, D., Handayani, L., Harinanto, G., Santoso, I., Sari, P.A., Rimainar, A.,
1004 2009. Bioequivalence Study with Two Naproxen Sodium Tablet Formulations in Healthy
1005 Subjects. J. Bioequivalence Bioavailab. -Open Access Res. Artic. JBB J Bioequiv Availab 1, 28–33.

1006 Shebley, M., Sandhu, P., Emami Riedmaier, A., Jamei, M., Narayanan, R., Patel, A., Peters, S.A., Reddy,
1007 V.P., Zheng, M., de Zwart, L., Beneton, M., Bouzom, F., Chen, J., Chen, Y., Cleary, Y., Collins, C.,
1008 Dickinson, G.L., Djebli, N., Einolf, H.J., Gardner, I., Huth, F., Kazmi, F., Khalil, F., Lin, J., Odinecs,
1009 A., Patel, C., Rong, H., Schuck, E., Sharma, P., Wu, S.-P., Xu, Y., Yamazaki, S., Yoshida, K.,
1010 Rowland, M., 2018. Physiologically Based Pharmacokinetic Model Qualification and Reporting
1011 Procedures for Regulatory Submissions: A Consortium Perspective. Clin. Pharmacol. Ther. 104,
1012 88–110.

1013 Sheng, J.J., McNamara, D.P., Amidon, G.L., 2009. Toward an In Vivo dissolution methodology: A
1014 comparison of phosphate and bicarbonate buffers. Mol. Pharm. 6, 29–39.

1015 Stillhart, C., Parrott, N.J., Lindenberg, M., Chalus, P., Bentley, D., Szepes, A., 2017. Characterising Drug
1016 Release from Immediate-Release Formulations of a Poorly Soluble Compound, Basmisanil,
1017 Through Absorption Modelling and Dissolution Testing. AAPS J. 19, 827–836.

1018 Suarez-Sharp, S., Cohen, M., Kesisoglou, F., Abend, A., Marroum, P., Delvadia, P., Kotzagiorgis, E., Li,
1019 M., Nordmark, A., Bandi, N., Sjögren, E., Babiskin, A., Heimbach, T., Kijima, S., Mandula, H.,
1020 Raines, K., Seo, P., Zhang, X., 2018. Applications of Clinically Relevant Dissolution Testing:
1021 Workshop Summary Report. AAPS J. 20, 93.

1022 Tubic-Grozdanis, M., Bolger, M.B., Langguth, P., 2008. Application of Gastrointestinal Simulation for
1023 Extensions for Biowaivers of Highly Permeable Compounds. AAPS J. 10, 213–226.

U.S.FDA Center for Drug Evaluation and Research (CDER), 2018a. Physiologically Based Pharmacokinetic Analyses — Format and Content Guidance for Industry.

U.S.FDA Center for Drug Evaluation and Research (CDER), 2018b. Physiologically Based Pharmacokinetic Analyses — Format and Content Guidance for Industry.

Upton, R., Williams, R., Kelly, J., Jones, R., 1984. Naproxen pharmacokinetics in the elderly. Br. J. Clin. Pharmacol. 18, 207–214.

Van den Ouweland, F.A., Jansen, P.A., Tan, Y., Van de Putte, L.B., Van Ginneken, C.A., Gribnau, F.W., 1988. Pharmacokinetics of high-dosage naproxen in elderly patients. Int. J. Clin. Pharmacol. Ther. Toxicol. 26, 143–7.

Vree, T.B., Van Den Biggelaar-Martea, M., Verwey-Van Wissen, C.P.W.G.M., Vree, J.B., Guelen, P.J.M., 1993. Pharmacokinetics of naproxen, its metabolite O-desmethylnaproxen, and their acyl glucuronides in humans. Biopharm. Drug Dispos. 14, 491–502.

Wang, J., Flanagan, D.R., 2002. General solution for diffusion-controlled dissolution of spherical particles. 2. Evaluation of experimental data. J. Pharm. Sci. 91, 534–542.

Wang, J., Flanagan, D.R., 1999. General solution for diffusion-controlled dissolution of spherical particles. 1. Theory. J. Pharm. Sci. 88, 731–738.

Wedagedera, J., Cain, T., Pathak, S.M., Jamei, M., 2017. Virtual Bioequivalence Assessment of Two Tramadol Formulations using the Advanced Dissolution Absorption and Metabolism (ADAM) Model via Simcyp R Package.

Yazdanian, M., Briggs, K., Jankovsky, C., Hawi, A., 2004. The “High Solubility” Definition of the Current FDA Guidance on Biopharmaceutical Classification System May Be Too Strict for Acidic Drugs. Pharm. Res. 21, 293–299.

Zhang, X., Wen, H., Fan, J., Vince, B., Li, T., Gao, W., Kinjo, M., Brown, J., Sun, W., Jiang, W.,

1047 Lionberger, R., 2017. Integrating *In Vitro* , Modeling, and *In Vivo* Approaches to Investigate
1048 Warfarin Bioequivalence. CPT Pharmacometrics Syst. Pharmacol. 6, 523–531.

1049 Zhao, P., Rowland, M., Huang, S.-M., 2012. Best practice in the use of physiologically based
1050 pharmacokinetic modeling and simulation to address clinical pharmacology regulatory
1051 questions. Clin. Pharmacol. Ther. 92, 17–20.

1052 Zhao, Y., Le, J., Abraham, M., Hersey, A., Eddershaw, P., Luscombe, C., Butina, D., Beck, G.,
1053 Sherborne, B., Cooper, I., Platts, J., 2001. Evaluation of human intestinal absorption data and
1054 subsequent derivation of a quantitative structure-activity relationship (QSAR) with Abraham
1055 descriptors. J. Pharm. Sci. 90, 749–784.

1056 Zhou, D., Zhang, Q., Lu, W., Xia, Q., Wei, S., 1998. Single- and multiple-dose pharmacokinetic
1057 comparison of a sustained-release tablet and conventional tablets of naproxen in healthy
1058 volunteers. J. Clin. Pharmacol. 38, 625–629.

1059

1060

8 List of Figures

9 List of Tables

1167 *Table 1: Composition and physicochemical characteristics of biorelevant media in the fasted and fed states.*

	Fasted state						Fed state		
	FaSSGF Level I	FaSSGF Level III	FaSSIF Level II	FaSSIF V3 Level I	FaSSIF V3 Level II	$FeSSGF_{middle}$ Level II	FeSSIF Level I	FeSSIF Level II	FeSSIF V2 Level II
Sodium Taurocholate (mM)	—	0.08	3.0	—	1,4	—	—	15	10
Sodium Glycocholate (mM)	—	—	—	—	1,4	—	—	—	—
Glyceryl monooleate (mM)	—	—	—	—	—	—	—	—	5
Sodium Oleate (mM)	—	—	—	—	0,315	—	—	—	0.8
Lecithin (mM)	—	0.02	0.75	—	0,035	—	—	3.75	2
Lysolecithin (mM)	—	—	—	—	0,315	—	—	—	—
Cholesterol (mM)	—	—	—	—	0,2	—	—	—	—
Pepsin (mg/mL)	—	0.1	—	—	—	—	—	—	—
Sodium dihydrogen phosphate (mM)	—	—	28.7	13,51	13,51	—	—	—	—
NaOH (mM)	—	—	13.8	3,19	3,19	—	101	101	102.4
Acetic acid (mM)	—	—	—	—	—	18.31	144	144	—
Maleic acid (mM)	—	—	—	—	—	—	—	—	71.9
Sodium acetate (mM)	—	—	—	—	—	32.98	—	—	—
Lipofundin®: buffer	—	—	—	—	—	8.75: 91.25	—	—	—
Hydrochloric acid	q.s. pH 1,6	q.s. pH 1,6	—	—	—	q.s. pH 5	—	—	—
Sodium chloride (mM)	—	34.2	106	—	91,62	181.7	—	204	125.5
Osmolality (mOsm/kg)	—	121	270	—	215	400	—	635	390
Buffer capacity (HCl) ((mmol/L)/ΔpH)	n.a.	n.a.	12	5,6	5,6	25	76	76	25
pH	1,6	1.6	6.5	6,7	6,7	5.0	5.0	5.0	5.8

1168 q.s.- quantum satis; n.a.- not applicable

1169

1170 *Table 2: Mean (SD) demographic data of in vivo studies used for the development and verification of the PBPK model. (HV= healthy*

1171 *volunteers)*

Reference	Formulation & Dose	N° of Subjects	Female Ratio	Ethnicity	Population	Age (y)	BW Range (kg)	BH Range (cm)
Intravenous								
(Runkel et al., 1973, 1972a, 1972b)	93 mg with 30µC tritium label in 100 mL phosphate buffer	3	0.33	Caucasian	HV	–	49.9-86.3	–
Oral								
(Charles and Mogg, 1994)	Naprosyn® 500 mg	16	0.125	Caucasian	HV	22.1 (4.4)	67.6 (8.3)	175.7 (9.0)
(Zhou et al., 1998)	Naprosyn® 2 x 250 mg	10	0	Chinese	HV	19-38	51-74	–
Haberer et al. (a)(Haberer et al., 2010)	Anaprox® 550 mg	8	0.63	Caucasian	HV	44.3 (8.5)	71.44 (12.3)	–
(Setiawati et al., 2009)	Anaprox® 550 mg	26	0.15	Caucasian	HV	19-46	–	–
(Rao et al., 1993)	IR Naproxen 500 mg	12	0	Indian	HV	18-22	46-62.5	160-182.5
Haberer et al. (b)(Haberer et al., 2010)	IR Naproxen-Na 500 mg	16	0.63	Caucasian	HV	44.3 (8.5)	71.44 (12.3)	–

1172

1173

1174

1175

1176 *Table 3: Input parameters for naproxen PBPK model development and simulations*

Parameters	Value	Reference/ Comments
Physicochemical & Blood Binding		
MW (g/mol)	230.3	PubChem
$logP_{o:w}$	3.2	(Bergström et al., 2014; Pérez et al., 2004; Zhao et al., 2001)
pKa	4.43	estimated from *in vitro* data (see section 3.2)
Blood/ Plasma ratio	0.55	(Brown et al., 2007)
Fraction unbound in plasma	0.01	(Davies and Anderson, 1997; Paixão et al., 2012)
Absorption		
Model	ADAM	
$P_{eff,\ human}$ ($x10^{-4}$ cm/s)	8.5	(Lennernas et al., 1995)
Formulation type	Immediate Release	
In vivo dissolution	see Table 7,Table 8	estimated DLM scalars from *in vitro* data (see section 3.3.2)
S_0 (mg/mL)	0.0294	*in vitro* data (see section 3.1)
Particle density (g/mL)	1.20	Default value within ADAM
Particle size distribution	Monodispersed	Assumed as data not available
Particle radius (µm)	10	Default value within ADAM
$logK_{m:w}$ neutral	5.37	estimated from *in vitro* data (see section 3.2)
$logK_{m:w}$ ion	4.00	estimated from *in vitro* data (see section 3.2)
Distribution		
Model	Minimal PBPK with SAC	
V_{ss} (L/kg)	0.15	PE module

V_{sac} (L/kg)	0.075	PE module
Q_{sac} (L/h)	1.00	PE module
Elimination		
CL_{iv} (L/h)	0.40	PE module
CL_{renal} (L/h)	0.02	(Paixão et al., 2012)

1177

1178

1179

1180 *Table 4: Mean (± SD) equilibrium solubility in aqueous media at 37°C for 24h (Uniprep® method).*

	Naproxen		Naproxen Sodium	
Aqueous medium	pH_{final}	Solubility (µg/mL)	pH_{final}	Solubility (µg/mL)
Water	4.5	70.4 (1.2)	6.7	358.4 (18.1)
HCl acid (pH=1.2)	1.3	29.4 (6.4)	1.2	28.4 (0.72)
Acetate buffer (pH=4.5)	4.5	84.8 (4.2)	4.6	103.1 (3.6)
Level I FeSSIF V1 (pH=5.0)	5.0	175.4 (0.0202)	5.1	241.6 (5.2)
Phosphate buffer (pH=6.5)	6.2	1627.6 (31.5)	6.6	2363.4 (31.5)
Phosphate buffer(pH=6.8)	6.5	3619.1 (112.6)	6.9	4957 (119)
Phosphate buffer (pH=7.4)	6.8	5981.6 (28.0)	7.5	10128 (674)

1181

1182

1183 *Table 5: Mean (± SD) equilibrium solubility in fasted and fed state biorelevant media at 37°C for 24h (Uniprep® method).*

	Naproxen		**Naproxen Sodium**	
Biorelevant medium	pH_{final}	Solubility (µg/mL)	pH_{final}	Solubility (µg/mL)
Fasted state				
Level III FaSSGF (pH=1.6)	1.6	33.4 (1.1)	1.6	31.8 (0.92)
Level II FaSSIF V1 (pH=6.5)	5.9	2046 (150)	6.5	3587 (179)
Level II FaSSIF V3 (pH=6.7)	5.8	1624 (153)	6.7	3469 (187)
Fed state				
Level II $FeSSGF_{middle}$ (pH=5.0)	4.9	352.6 (21.4)	5.1	575.2 (19.3)
Level II FeSSIF V1 (pH=5.0)	5.0	424.7 (26.6)	5.0	519.9 (18.9)
Level II FeSSIF V2 (pH=5.8)	5.8	890.0 (56.7)	5.8	799.5 (177)

1184

1185

Table 6: Parameter estimates (95% CI) resulting from the model-based analysis of in vitro solubility data in aqueous as well as biorelevant media. The pka was estimated from the aqueous solubility values, whereas for the micelle-water partition coefficients (log$K_{m:w}$ neutral, ion) estimation, biorelevant solubilities were used. The accuracy of the predictions was evaluated with the R squared.

	pKa	log$K_{m:w}$ neutral	log$K_{m:w}$ ion
Estimate (95% CI)	4.43 (4.42-4.44)	5.37 (5.34-5.40)	4.00 (3.98-4.02)
R^2	0.9990	0.9999	

Table 7: Estimated DLM scalar values (95% CI) obtained from model-based analysis of in vitro dissolution in various media of naproxen free acid and sodium salt pure API powder. The goodness of fit between predicted and observed dissolution profiles was evaluated with the R squared (R^2).

Dissolution Medium	**API Powder**	
	NPX	**NPX Na**
Level I FaSSIF V3		
DLM (95% CI)	0.0022 (0.0021-0.0023)	1*
R^2	0.997	–
Eur. Phar. Phosphate Buffer (pH=6.8)		
DLM (95% CI)	0.0136 (0.0121-0.0151)	1*
R^2	0.992	–
Level II FaSSIF V3		
DLM (95% CI)	0.0810 (0.0651-0.0970)	1*
R^2	0.998	–

* default values of DLM scalar due to very fast dissolution (>85% dissolved in 2.5 min)

Table 8: Estimated DLM scalar and first-order disintegration rate constant (k_d) values (95% CI) obtained from model-based analysis of in vitro dissolution in various media of naproxen free acid (Naprosyn®) and sodium salt (Anaprox®) formulation. In case of dissolution without pre-treatment in a gastric medium, a first-order disintegration model was included. The goodness of fit between predicted and observed dissolution profiles was evaluated with the R squared (R^2).

Dissolution Medium	**Formulation**	
	Naprosyn	**Anaprox**
Level I FaSSIF V3		
DLM (95% CI)	0.0296 (0.0149-0.0443)	0.0212 (0.0131-0.0294)
kd (95% CI)	0.305 (0.123-0.487)	0.288 (0.130-0.446)
R^2	0.999	0.998
Level I FaSSIF V3 (two-stage)		
DLM (95% CI)	0.0305 (0.0191-0.0308)	0.0221 (0.0174-0.0267)
kd (95% CI)	–	–
R^2	0.967	0.981
Level II FaSSIF V3		
DLM (95% CI)	0.0213 (0.0170-0.0255)	0.0168 (0.00996-0.0237)
kd (95% CI)	0.702 (0.354-1.05)	0.228 (0.0975-0.358)
R^2	0.999	0.999
Level II FaSSIF V3 (two-stage)		
DLM (95% CI)	0.0187 (0.0143-0.0230)	0.0158 (0.0138-0.0179)
kd (95% CI)	–	–
R^2	0.975	0.991

1202

1203

Table 9: Mean in silico population pharmacokinetic (popPBPK) parameters of naproxen simulated plasma-concentration-time profiles under all tested in vivo dissolution inputs (DLM scalar values) as obtained from model-based analysis of the in vitro data (see formulation and dissolution medium).

Formulation	Medium	S_{DLM}	Disintegration	*In silico* mean popPBPK parameters		
			kd (h^{-1})/2-stage	t_{max} (h)	C_{max} (mg/L)	AUC (mg/L·h)
API						
Naproxen						
	Level I FaSSIF V3	0.0022	–	2.52	65.5	1302
	Ph. Eur. Phosphate	0.0136	–	1.80	69.0	1305
	Level II FaSSIF V3	0.0810	–	1.44	69.4	1306
Naproxen Na						
	all media	1	–	1.44	69.6	1306
Formulation						
Naprosyn						
	Level I FaSSIF V3	0.0396	0.305	1.80	67.5	1277
		0.0305	2-stage	1.80	69.2	1306
	Level II FaSSIF V3	0.0213	0.702	1.80	67.8	1277
		0.0187	2-stage	1.80	69.1	1306
Anaprox						
	Level I FaSSIF V3	0.0212	0.288	1.80	67.9	1277

		0.0221	2-stage	1.80	69.2	1306
	Level II FaSSIF V3	0.0168	0.228	1.80	67.7	1277
		0.0158	2-stage	1.80	69.1	1305

1207

1208

Table 10: Mean (SD) pharmacokinetic parameters of naproxen in vivo studies ([a] Median value).

Reference	Formulation & Dose	*In vivo* mean PK parameters (SD)		
		t_{max} (h)	C_{max} (mg/L)	AUC (mg/L·h)
(Charles and Mogg, 1994)	Naprosyn® 500 mg	1.50[a]	71.4[a]	1211[a]
(Zhou et al., 1998)	Naprosyn® 2 x 250 mg	2.6 (1.5)	87.3 (15.5)	1428 (193)
(Haberer et al., 2010)	Anaprox® 550 mg	1.48	75.2	1294
(Setiawati et al., 2009)	Anaprox® 550 mg	1.00 (0.5-2)	72.0 (11.2)	1013 (186)
(Rao et al., 1993)	IR Naproxen 500 mg	1.36 (0.81)	69.2 (20.9)	1435 (312)
Haberer et al. (b)(Haberer et al., 2010)	IR Naproxen-Na 500 mg	1.53	74.9	1299

Table 11: Mean in silico population pharmacokinetic (popPBPK) parameters of naproxen virtual clinical trials for the hypothetical reference and test formulations prior to bioequivalence assessment.

Trial N°	*In silico* mean popPBPK parameters					
	Reference			Test		
	t_{max} (h)	C_{max} (mg/L)	AUC (mg/L·h)	t_{max} (h)	C_{max} (mg/L)	AUC (mg/L·h)
1	1.66	62.01	1249	2.26	57.66	1248
2	1.51	65.79	1275	2.31	62.58	1273
3	1.96	61.30	1624	2.59	59.67	1623
4	1.58	74.97	1659	2.41	70.61	1657
5	1.75	60.35	1785	2.84	55.14	1783
6	1.55	72.27	1404	2.56	67.34	1403
7	1.45	64.14	1426	2.02	62.17	1425
8	1.39	71.03	1473	2.47	65.14	1472
9	1.58	61.87	1340	2.26	58.88	1339
10	1.64	62.32	1348	2.39	60.46	1347

1216 Figure 1:

1217

1218

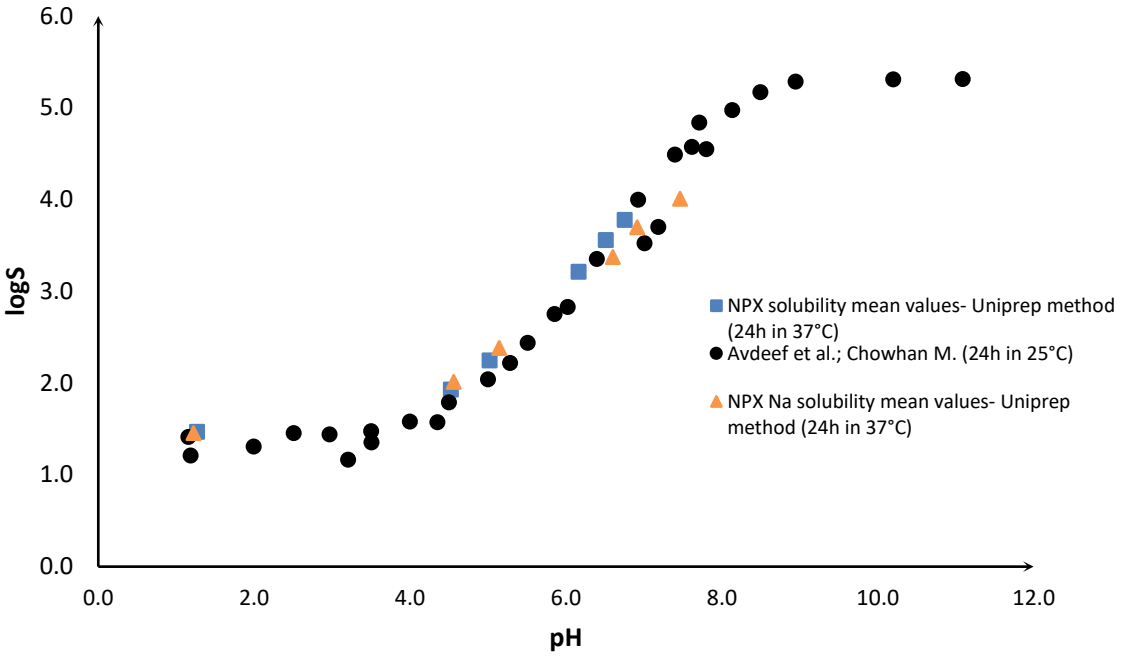

1219

1220 Figure 2:

1221

1222

1223

1224

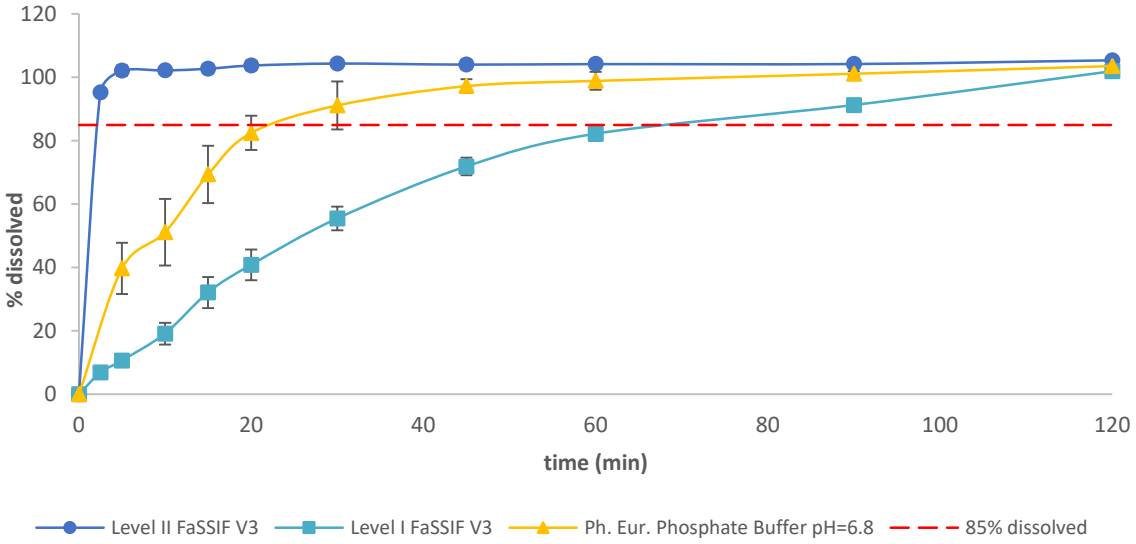

1225 Figure 3:

1226

1227

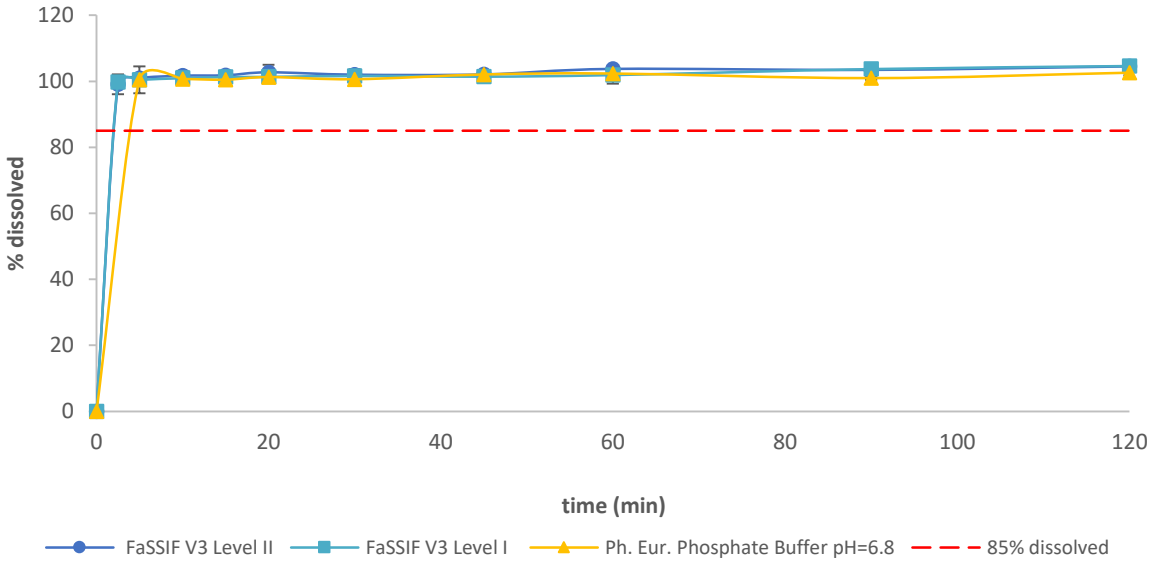

1228

1229 Figure 4:

1230

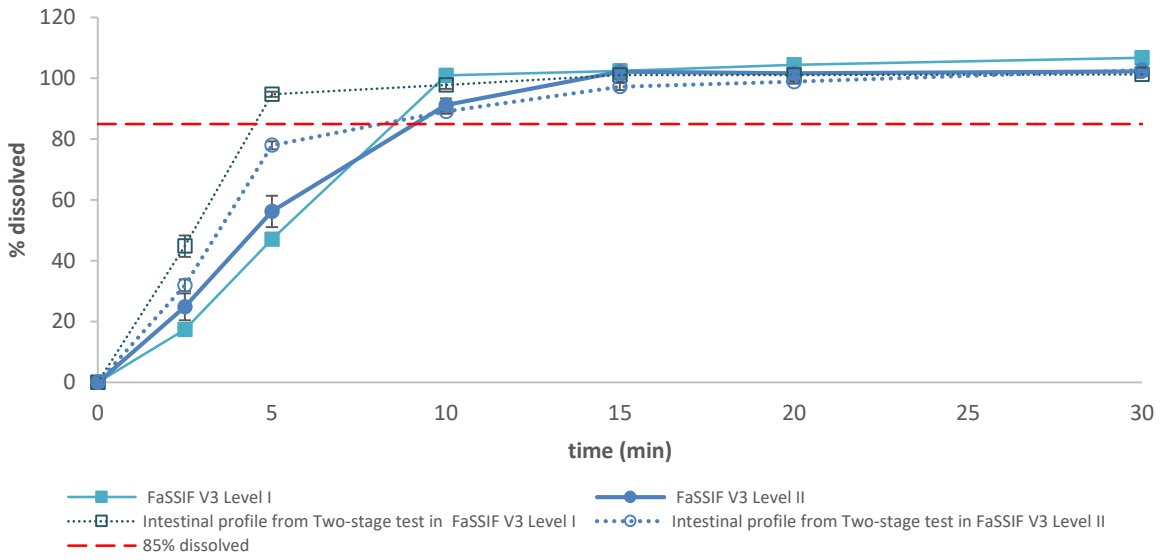

1231

1232

1233

1234 Figure 5:

1235

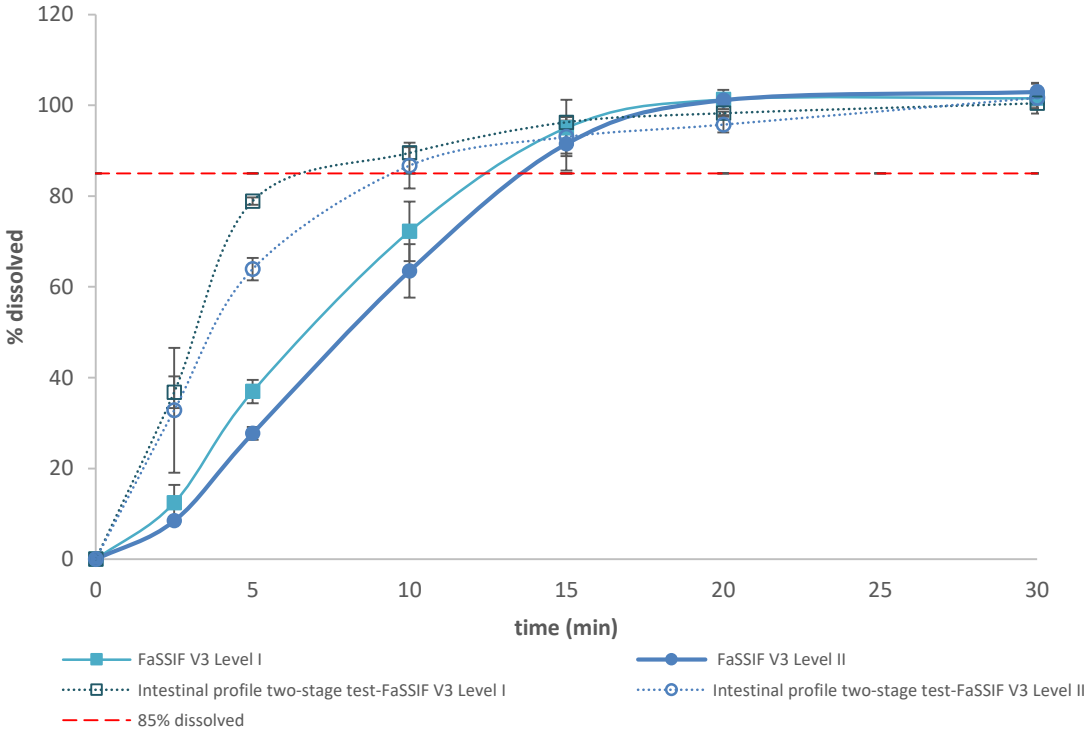

1236

1237

1238

Figure 6:

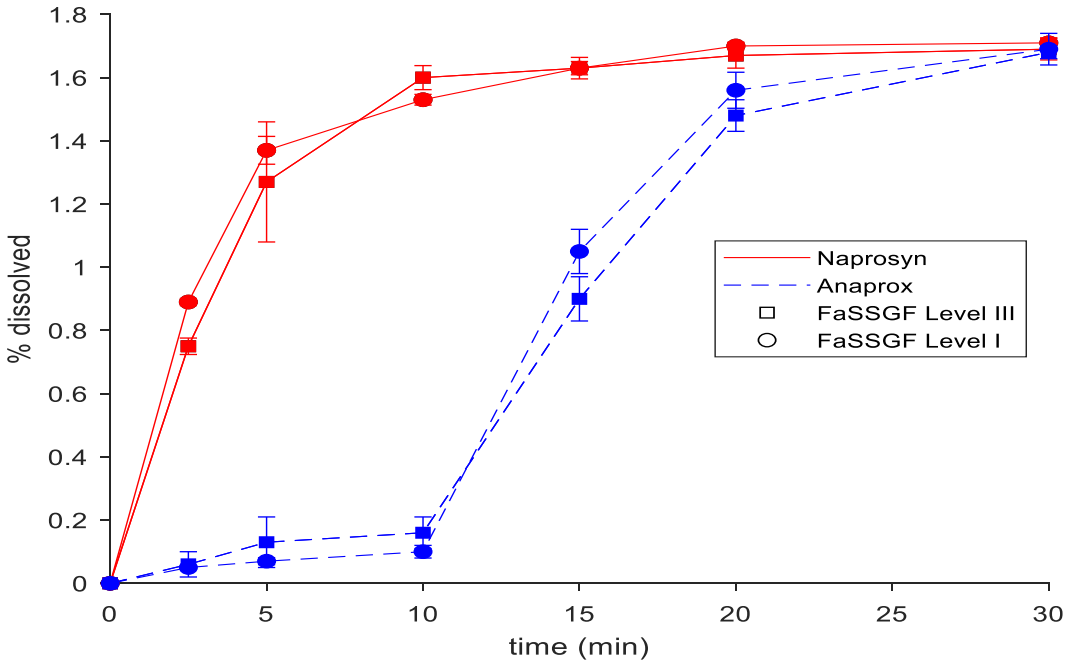
1.8
1.6
1.4
1.2
1
0.8
0.6
0.4
0.2
0
% dissolved
0
5
10
15
20
25
30
time (min)
Naprosyn
Anaprox
FaSSGF Level III
FaSSGF Level I

1248 Figure 7:

1249

1250

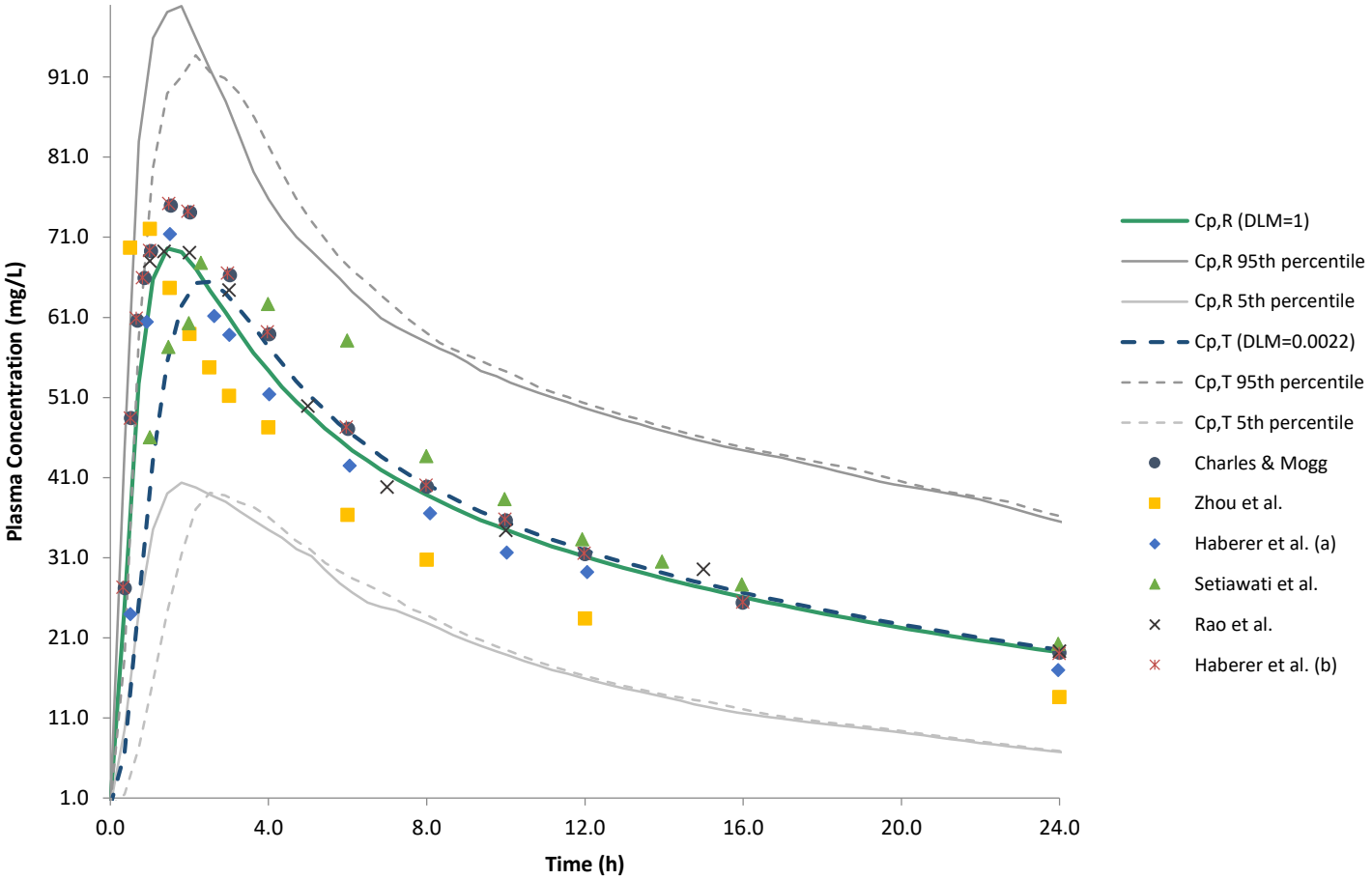

1251

1252

1253

1254 Figure 8:

1255

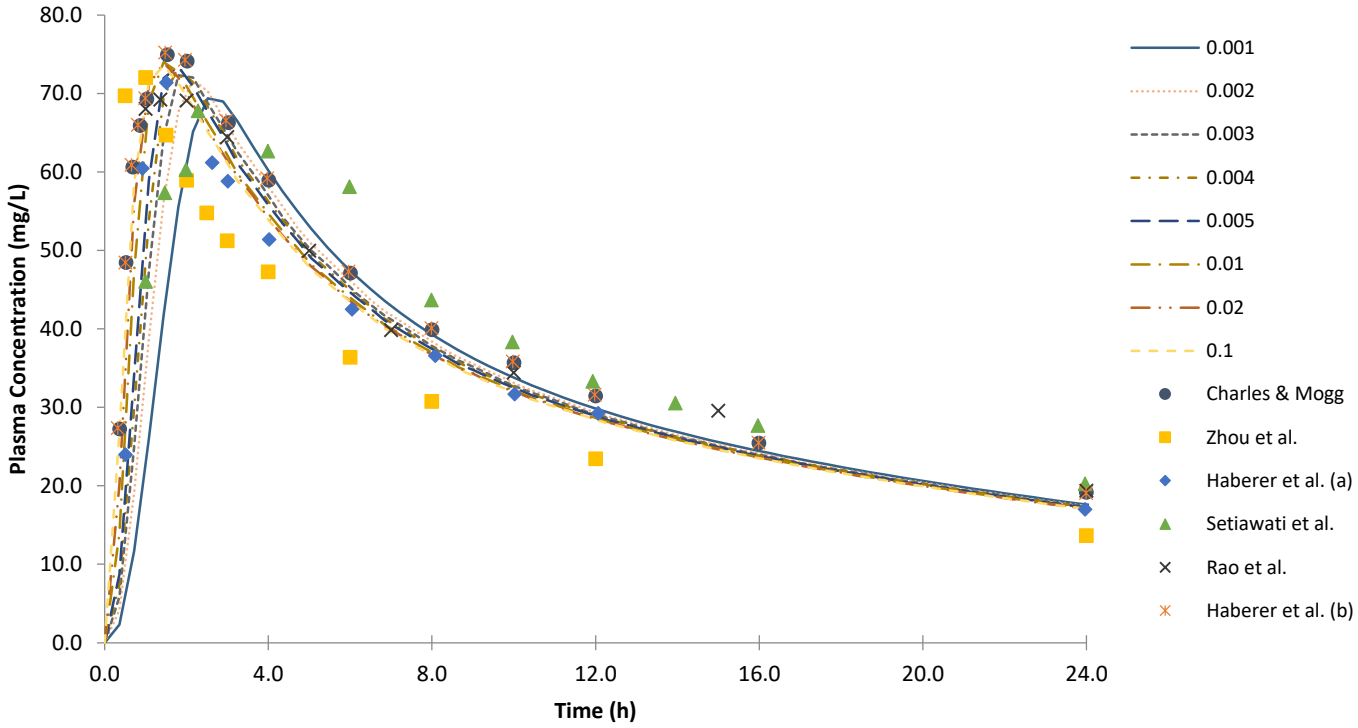

1256

1257

1258 Figure 9:

1259

1260

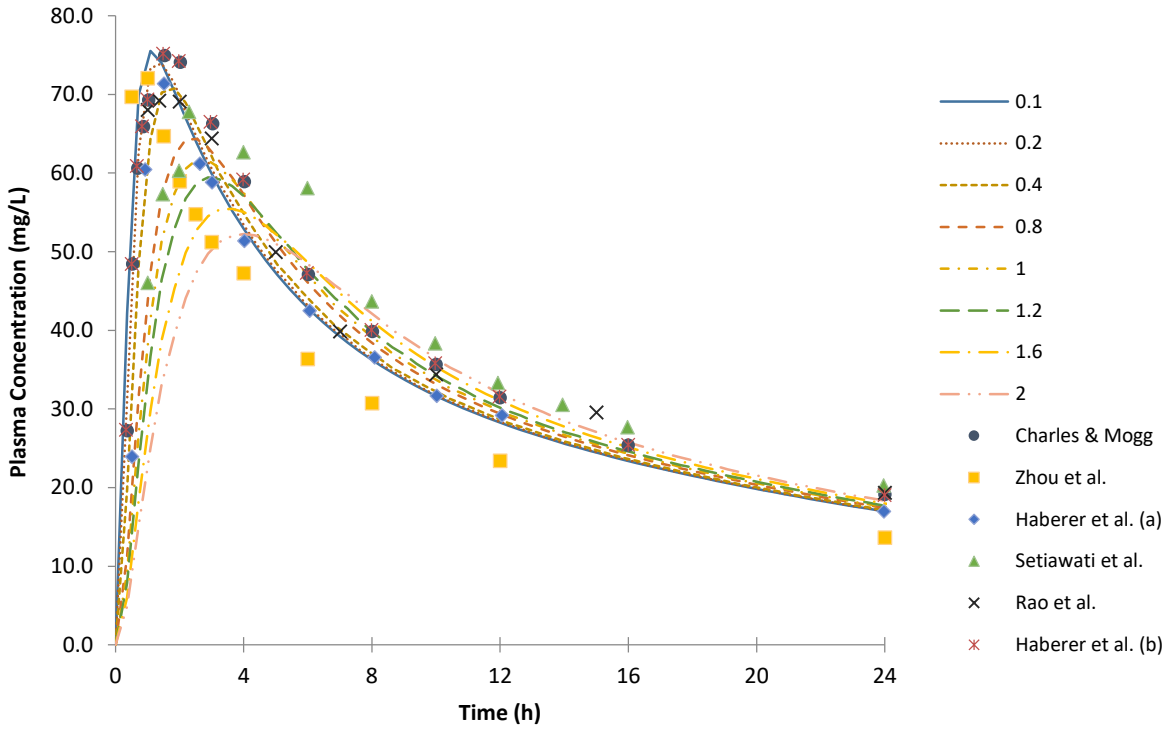

1261

1262

1263

Figure 10:

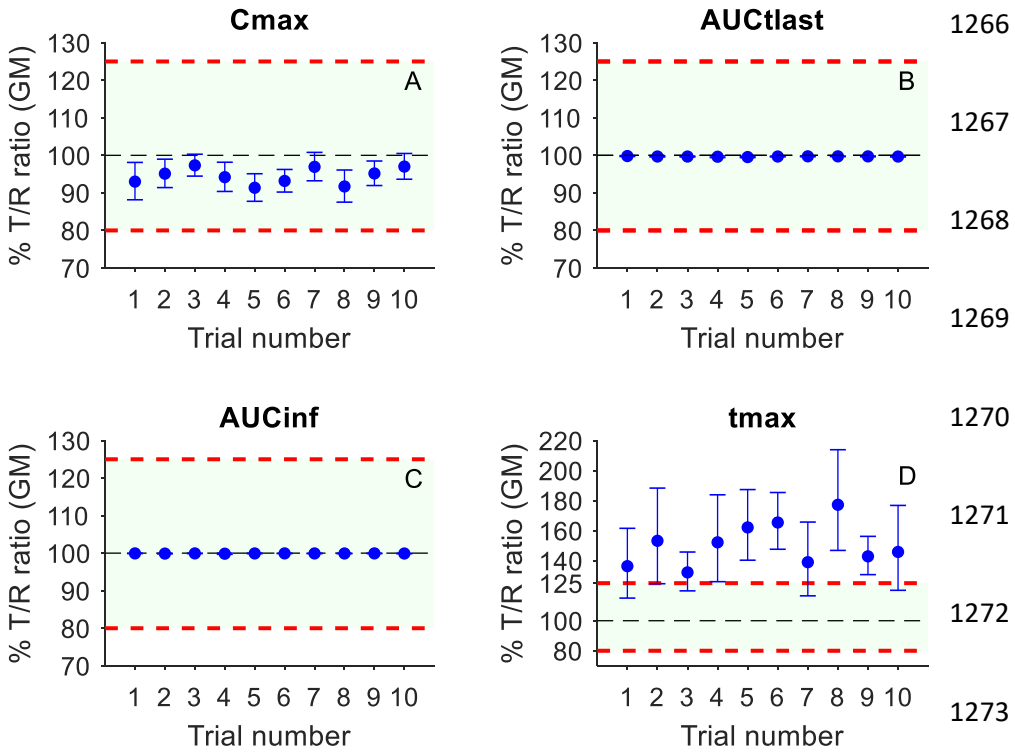
Cmax
A
% T/R ratio (GM)
130
120
110
100
90
80
70
1 2 3 4 5 6 7 8 9 10
Trial number
AUCtlast
B
% T/R ratio (GM)
130
120
110
100
90
80
70
1 2 3 4 5 6 7 8 9 10
Trial number
AUCinf
C
% T/R ratio (GM)
130
120
110
100
90
80
70
1 2 3 4 5 6 7 8 9 10
Trial number
tmax
D
% T/R ratio (GM)
220
200
180
160
140
125
100
80
1 2 3 4 5 6 7 8 9 10
Trial number

1280 Figure 11:

1281

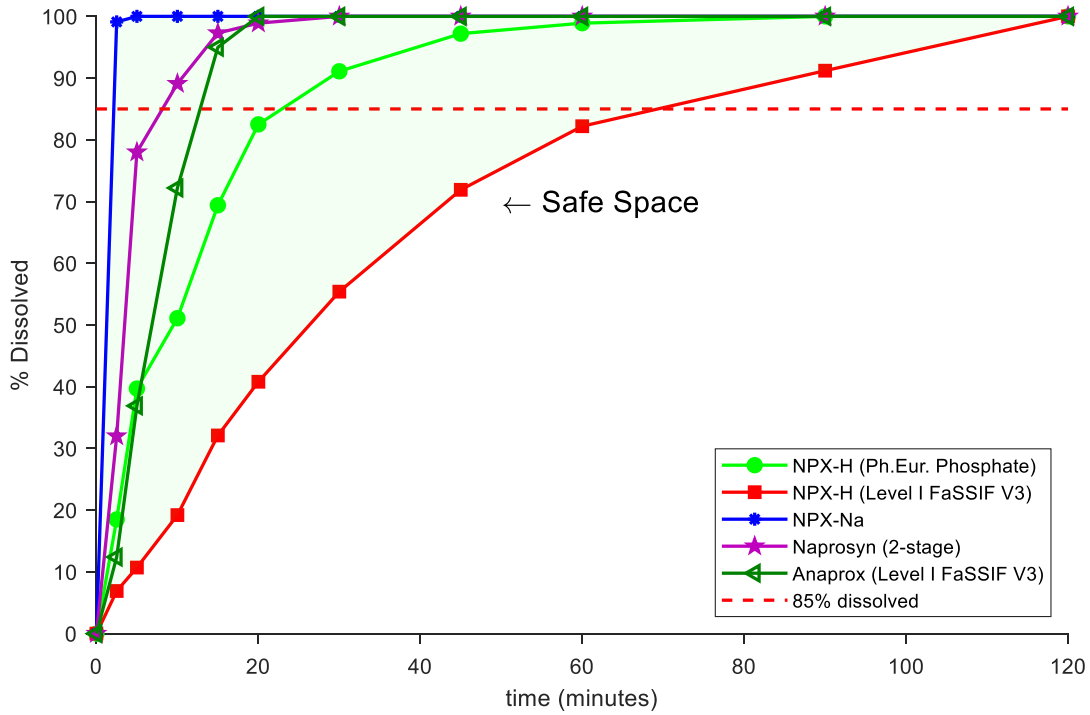

1282